

# The X-ray emission of the $\gamma$ Cassiopeiae stars

Myron A. Smith

*National Optical Astronomical Observatory, 950 N. Cherry Ave., Tucson, AZ, U.S.A.*

R. Lopes de Oliveira

*Universidade Federal de Sergipe, Departamento de Física, Av. Marechal Rondon, S/N, 49000-000 São Cristóvão, SE, Brazil; Observatório Nacional, Rua Gal. José Cristino 77, 20921-400, Rio de Janeiro, RJ, Brazil*

C. Motch

*Observatoire Astronomique, Université de Strasbourg, CNRS UMR7550, 11 rue de l'Université, F-67000, Strasbourg, France*

---

## Abstract

Long considered as the “odd man out” among X-ray emitting Be stars,  $\gamma$  Cas (B0.5eIV) is now recognized as the prototype of a class of stars that emit hard thermal X-rays. Our classification differs from the historical use of the term “ $\gamma$  Cas stars” defined from optical properties alone. The luminosity output of this class contributes significantly to the hard X-ray production in massive stars in the Galaxy. The  $\gamma$  Cas stars have light curves showing variability on a few broadly-defined timescales and spectra indicative of an optically thin plasma consisting of one or more hot thermal components. By now 9–13 Galactic  $\approx$ B0-1.5e main sequence stars are judged to be members or candidate members of the  $\gamma$  Cas class. Conservative criteria for this designation are for a  $\approx$ B0-1.5e III-V star to have an X-ray luminosity of  $10^{32}$ – $10^{33}$  ergs s $^{-1}$ , a hot thermal spectrum containing the short wavelength Ly $\alpha$  Fe XXV and Fe XXVI lines and the fluorescence FeK feature all in emission. If thermality cannot be demonstrated, for example from either the presence of these Ly $\alpha$  lines or curvature of the hard continuum of the spectrum of an X-ray active Be star, we call them  $\gamma$  Cas *candidates*. We discuss the history

---

*Email addresses: masmith@noao.edu (Myron A. Smith), rlopes@ufs.br/ (R. Lopes de Oliveira), christian.motch@unistra.fr (C. Motch)*

of the discovery of the complicated characteristics of the variability in the optical, UV, and X-ray domains, leading to suggestions for the physical cause of the production of hard X-rays. These include scenarios in which matter from the Be star accretes onto a degenerate secondary star and interactions between magnetic fields on the Be star and its decretion disk. The greatest aid to the choice of the causal mechanism is the temporal correlations of X-ray light curves and spectra with diagnostics in the optical and UV wavebands. We show why the magnetic star-disk interaction scenario is the most tenable explanation for the creation of hard X-rays on these stars.

*Keywords:* stars: individual, stars: massive, stars: emission-line Be, stars: X-ray

---

## 1. Introduction: description of $\gamma$ Cas as an X-ray emitter.

### 1.1. Early X-ray discoveries.

Discovered as the first star to show Balmer line emission in its spectrum (Secchi, 1866),  $\gamma$  Cas has long been held out as *the prototype* for what became known by the mid-20th century as a large class of “classical Be” variables.<sup>1</sup> However, with the discovery of anomalously high X-ray flux from the direction of this star (Jernigan, 1976; ?), it eventually was revealed that it is not a typical Be star after all - Be stars at large emit at most a few times more soft X-ray flux than normal B stars (Cohen, 2000), ostensibly due to shock interactions in their intermediate latitude hot winds. As we will see, the study of the generation of hard X-rays from a class of so-called “ $\gamma$  Cas stars” links a wide field of astrophysical subdisciplines. In addition, Motch et al. (2007, “M07”) and Nebot Gómez-Morán et al. (2013, “N13”) have noted that  $\gamma$  Cas stars contribute very significantly to the X-ray flux emitted from Galactic massive stars. This makes them relevant to an understanding of the energy budget of the interstellar medium (ISM) as well as the evolu-

---

<sup>1</sup>Classical Be stars are main sequence or giant B stars whose spectra have shown Balmer line emission and have shown no evidence of either recent binary interactions or star formation. These stars occasionally expel matter to a centrifugally supported, thin disk, with a small opening angle, e.g., (?). The presence of disks is heralded by emission in the lower Balmer spectral lines. Our use of the term “ $\gamma$  Cas stars” is distinct from the definition given in the General Catalog of Variable Stars, e.g., Samus et al. (2014), and is framed within the context of X-ray characteristics, as discussed herein.

tionary consequences of noncataclysmic expulsions of matter from Be binary systems.

The saga begins with the discovery that  $\gamma$  Cas is not just an X-ray source but a copious emitter of hard X-rays (White et al., 1982). This realization started something of a cottage industry aimed to develop an understanding of the mechanisms behind its surprising X-ray properties. The initial concept, which had been successfully applied to the generation of high energy for almost all high mass X-ray Be binary stars, is that the X-rays result from synchrotron emission (for a strongly magnetic secondary) and/or thermalization of accreted matter onto the surface, accretion column, or accretion disk hosted by a degenerate companion. In any of these scenarios the high energy emission ultimately results from the deep gravitational potential of the degenerate secondary. White et al. professed “little doubt” that  $\gamma$  Cas is a Be-NS (neutron star) system similar to the well known X-ray pulsar X Per. The reason for this judgment was that the light curve showed in their words a “factor of 2 quasi-periodic variations on a timescale similar to the pulsations from X Per.” Here they anticipated a timescale of 13.9 minutes, which is the pulse period in this X-ray pulsar. In addition, White et al. rejected coronal and white dwarf (WD) accretion mechanisms. In the latter case they made this judgment because the X-ray luminosity was considered too high for WD accretion, according to the mass loss rate estimated for  $\gamma$  Cas. Despite these arguments it soon became clear that  $\gamma$  Cas is not just another example of a Be-NS system.

### 1.2. Recent discoveries of X-ray properties.

By the end of the 20th century new generations of X-ray satellites provided data with improved spectral and time resolution. These data clarified the X-ray properties of  $\gamma$  Cas and a small number of “analog” members of this class and also established that the spectra were thermal and optically thin in nature. Also, the amassing of new light curves could not corroborate claims of persistent periodicities. Breakthroughs in evaluating the X-ray characteristics came from the advent of the *Rossi X-ray Timing Explorer (RXTE)* satellite, with its design purpose of providing reliable high time resolution light curves through the use of its six detectors comprising the *Proportion Counter Array (PCA)*, and from the appearance of *Chandra* and *XMM-Newton* satellites equipped with high resolution spectrometers sensitive to soft-to medium band flux (which we define somewhat arbitrarily as  $\lesssim 3$  keV, i.e.,  $\gtrsim 4$  Å).

The new generation light curves demonstrated that flux variability occurs on four basic timescales: rapid (seconds to a minute), intermediate (a few hours), long (a few months), and episodic (years). Meanwhile, results from turn-of-the-century X-ray spectrometers have indicated that the X-ray spectra are *basically* thermal. We clarify the qualifier “basically” as follows. First, one finds the continuum and the Lyman  $\alpha$  lines of Fe XXV (1.85 Å) and Fe XXVI (1.78 Å) can be fit well to a primary optically thin plasma component described by a single hot energy temperature, which we will call  $kT_{\text{hot}}$ . Second, the soft X-ray domain X-ray continuum suffers photoelectric absorption, which can be modeled by the equivalent of a hydrogen column density (hereafter  $N_{\text{H}}$ ), which is mainly attributable to the ISM as well as a local one  $N_{\text{H}_b}$  along the sight line to the hot plasma component. In addition, a number of emission lines in the soft X-ray waveband indicate the presence of additional cooler optically thin plasma components. If the spectral coverage is limited only to the hard X-ray region the continuum alone, one can determine a reasonably accurate value of  $kT_{\text{hot}}$  – but not necessarily also model the absorption column density. This is particularly true if one does not anticipate the possibility of multiple absorption columns. In such cases both the determination of  $kT_{\text{hot}}$  and the description of the column absorptions can be badly compromised (Smith et al., 2004, “S04”).

Given these properties,  $\gamma$  Cas has become a compelling mystery object with more than enough surprises to attract considerable interest within the stellar X-ray community (Güdel & Nazé, 2009). In the intervening time only some of the answers we now have as to how and where the hard X-rays are created can be attributed to the latest generation of X-ray satellites. Rather, crucial new information has come with temporal correlations of contemporaneous X-ray, optical, and UV data.

### 1.3. General properties.

#### 1.3.1. Stellar properties.

Apart from its X-ray emission,  $\gamma$  Cas appears to be a typical B0.5 IVe star. Its luminosity class IV is consistent with its being a field main sequence B star and having an age of  $\geq 15$ –20 Myr. Herein we will assume that  $\gamma$  Cas has a mass near  $15 M_{\odot}$ , a revised Hipparcos distance of 168 pc (van Leeuwen, 07), a radius of  $10 R_{\odot}$ , and an effective temperature  $T_{\text{eff}} = 28$  kK. With these parameters the uniform stellar disk diameter on the sky corresponds to 0.44 milliarcseconds (Stee et al., 2012). Robotic observations with the 16-inch “T3” Automated Photometric Telescope (APT) using the Johnson  $B$  and  $V$

filters consistently for more than 15 years indicate the presence of a robust signature with a period of  $1.215811 \pm 0.000030$  days (Henry & Smith, 2012, “HS12”), which is interpreted as the rotational period of  $\gamma$  Cas. Indeed, when one combines the 1.2 day period with the obliquity of the star/disk system (about  $45^\circ$ ) from Long Baseline Optical Interferometry or “LBOI” (Stee et al., 2012) one can reconcile the  $v \sin i$  value from spectral line broadening with the critical velocity at the equator for a B0.5 IV star.

### 1.3.2. Circumstellar disk measurements.

Because its  $H\alpha$  line exhibits strong, generally double-peaked, emission, it is clear that  $\gamma$  Cas hosts a flattened circumstellar “decretion” disk. The emission has been present for most all of its nearly 150 year observed history. A chronicle of the variations during the early and mid-20th century has been given by Doazan et al. (1983) and Harmanec (2002). These authors noted that the star’s  $H\alpha$  emission has not always been detectable, and in fact it disappeared during 1942–1946 after a brief period of “spectacular variations” (SV). Although many astronomers believe these variations are due to internal instabilities rising to the Be star’s surface, Hummel (1998) has attributed them to the precession of the Be disk that is tilted with respect to the star’s equatorial plane. However for such an explanation to hold, the orientation of the disk would have to change, and thus depart from the rotational plane, at the start and end of the SV era. The observational techniques needed to determine disk coplanarity were not developed at that time.

In recent history this emission has been more or less slowly building since a sudden outburst in 1969. Documentations of the  $H\alpha$  emission have been carried out, albeit with heterogeneous instruments since 1991, and with a single stable low-resolution spectrographic-CCD system since late 1994 (Pollmann, 2014; Smith et al., 2012, “S12”). These observations showed the existence of a quasi-periodicity of the Violet/Red emission ratio extending over the last three decades of the 20th century, but this cyclicity had disappeared by 2000. Sigut & Jones (2007) have published a self-consistent model for the  $\gamma$  Cas disk that assumes both radiative-equilibrium and an axisymmetric geometry. These authors found a volume density at the equatorial disk base of  $3\text{--}5 \times 10^{-11} \text{ g cm}^{-3}$ , similar to earlier results by Millar, Sigut, & Marlborough (2000). The latter paper gives a vertical column density at the base of  $0.2 \text{ g cm}^{-2}$  ( $10^{23} \text{ atoms cm}^{-2}$ ).

The circumstellar disk of  $\gamma$  Cas has been resolved by a number of LBOI studies. The best models for the visibility functions are consistent with the

geometry of an ellipsoid with a Gaussian drop-off in density. In addition to LBOI observations centered on the  $H\alpha$  line, observations have been carried out across various continuum bands, including  $V$ , “near  $H\alpha$ ,” and infrared  $H$  and  $K$  bands ( $1.85\ \mu\text{m}$  and  $2.1\ \mu\text{m}$ , respectively). Brief histories of LBOI studies of this star/disk system can be found in [Thom, Granès & Vakili \(1986\)](#), [Quirrenbach et al. \(1997\)](#), [Stee \(1996\)](#), [Tycner et al. \(2006\)](#), [Gies et al. \(2007\)](#), and [Stee et al. \(2012\)](#). These studies give important constraints on the structure of the inner disk of  $\gamma$  Cas, including its opening angle and density drop-off with radius. These results also demonstrate that the spatial extent of  $\gamma$  Cas’s disk in the sky increases at long wavelengths. This is in agreement with the expectation that infrared continuum radiation of the disk is dominated by bound-free emission and thus become more optically thick at these wavelengths. [Berio et al. \(1999\)](#) used time-resolved LBOI in  $H\alpha$  to track prograde precession of a one-arm density wave embedded in the disk. In addition, LBOI observations attached to a high dispersion spectrograph have shown that the disk obeys a Keplerian rotation law around the Be star out to the outer limits of its detectability ([Meilland et al., 2011](#); [Stee et al., 2012](#)). Note, however, that these data do not constrain the rotation rate of the inner disk, that is to within about one stellar radius of the surface of the Be star.

### *1.3.3. Description of binary orbit.*

The radial velocity curve for the  $\gamma$  Cas binary system has been determined from monitoring the wavelengths of selected points on the  $H\alpha$  profile. Subtle changes in this profile can produce errors in the shape of the RV curve, making it challenging to measure the star’s radial velocity accurately. Nonetheless, it is now clear that the system has an orbital period of  $203.55\pm 0.20$  day, a full velocity amplitude  $2K = 7\ \text{km s}^{-1}$ , an eccentricity of  $\leq 0.03$ , and a secondary mass near  $0.8 M_{\odot}$  ([Harmanec et al., 2000](#); [Miroshnichenko, Bjorkman & Krugov, 2002](#); [Nemravová et al., 2012](#); [Smith et al., 2012](#)). Given these parameters the orbital separation of the two stellar components is  $36.5 R_{*}$  and the Roche lobe of the Be star is  $21.4 R_{*}$ , i.e., well beyond the observable outer edge of the circumstellar disk. It is also thought that the outer disk edge is truncated by 3:1 period resonances with the secondary star ([Okazaki & Negueruela, 2001](#)). The practical effect of this is not to create a sudden cut-off at this radius but rather to greatly steepen the density distribution beyond this point ([Okazaki et al., 2002](#)). From this consideration the accretion of matter will be at least somewhat diminished, thereby arguing against

an explanation involving X-ray emission from an accreting degenerate companion..

## 2. High Resolution X-ray Spectroscopy

We begin our detailed description of the phenomenological properties of the X-ray emitting plasmas, by discussing the analysis of high resolution spectroscopic data.

### 2.1. *Discovery of multiple thermal plasma components.*

Prior to the launches of *Tenma*, *Ginga*, and *BeppoSax* during the period 1983–1996, various studies had lacked the energy coverage and resolution to differentiate a thermal from a power law model in the  $\gamma$  Cas energy spectrum. These instruments as well as *Chandra* and *XMM-Newton* that followed them in 1999 showed the dominant plasma component has an energy temperature  $kT_{\text{hot}} \approx 12\text{--}14$  keV (i.e.,  $1.4\text{--}1.6 \times 10^8$  K). Significantly, [Murakami et al. \(1986, “M86”\)](#) discovered the presence of the Fe XXV and Fe XXVI lines in the X-ray spectrum, which although they are blended is important because they strongly suggest the spectrum is thermal and optically thin, and therefore that it is not formed by accretion onto a NS.

The first high resolution spectrum of  $\gamma$  Cas was obtained in August 2001, through the *Chandra* High Energy Transmission Grating spectrometer (S04). This spectrum covered the wavelength range  $1.6\text{--}25$  Å and immediately revealed surprises. Foremost among them was its steep gradient with wavelength. This was due only partly to the already high expected energy temperature of the dominant plasma. The remaining cause of this steep slope was the intervening high local column density that was present at this time. The low photon count rate near the short wavelength edge and the absorption column rendered an accurate determination of the temperature uncertain, so a value of 12.3 keV was adopted from an earlier analysis of the *BeppoSax* spectrum ([Owens et al., 1999](#)). However additional optically thin thermal components were needed in the modeling to explain the presence of Lyman  $\alpha$  emission lines arising from even-Z intermediate elements. In particular, towards longer wavelengths it became necessary to add plasma components of lower temperatures. In all S04 found that four components were required for a spectrum obtained in 2001, as S12 also found for spectrum obtained in 2010. [Lopes de Oliveira, Smith, & Motch \(2010, “L10”\)](#) had a slight preference for three components for a spectrum taken in 2004. The hot component,

with  $kT_{\text{hot}} \approx 12.3$  keV, was found to be responsible for 80–88% of the X-ray flux in the 0.2–10 keV energy band.<sup>2</sup> Recent *XMM/EPIC* (European Photon Imaging Camera) spectra, which provide moderate resolution coverage for wavelengths 1–41 Å, have pointed to similar  $kT_{\text{hot}}$  values, in particular 13.5–15.7 keV for four observations distributed over 40 days in 2010 (S12). However, it is not clear that the plasma temperature is changed over this short timescale because [Lopes de Oliveira, Smith, & Motch \(2010\)](#) found a similar range of values,  $kT_{\text{hot}} = 12.4$ – $14.3$  keV, for a single *XMM* observation made in 2004, though modeled with different analysis software. In all, while there may be some variation of the temperature of the primary plasma component, its documented variation is no larger than 2 keV.

Additional *XMM* spectra of  $\gamma$  Cas were obtained in February 2004 (L10) and July–August, 2010 (S12). Importantly, these observations were not just made through the European Photon Imaging Camera (EPIC) *pn* system (and in the latter case also the MOS1/MOS2 camera). The two Reflection Grating Spectrometers (RGS1/RGS2), which cover emission over 6.2–38 Å at high resolution. Also, the long-wavelength limit of the RGS system allows generous coverage of the soft X-ray regime. This means a better modeling of photoelectric absorption columns than *Chandra/HTEG* as well as the inclusion of emission lines arising from hydrogenic CNO ions as well as so-called “*rif*” triplets discussed in §2.3. These studies also showed a preference for three, or more probably four, optically thin plasma components. S12 also found that a continuous Differential Emission Measure (DEM) model gave a poorer fit to the data, meaning that the spectrum could indeed be best fit with plasmas having 3–4 discrete plasmas having different temperatures – not a single broad distribution of temperatures. Similar to earlier colorimetric monitoring studies using the *Rossi X-ray Time Explorer (RXTE)* satellite by [Smith, Robinson & Corbet \(1998, “SRC98”\)](#) and [Robinson & Smith \(2000, “RS00”\)](#), the temperature of the dominant (hot) plasma from  $\gamma$  Cas exhibits little epoch-to-epoch variation. Of the components found for a four component model, the third (having  $kT_{\text{warm},2} = 2.5$ – $4$  keV) usually has the smallest emission measure. Even so, its presence is essential for the formation of Fe L shell and other lines. S12 found that the temperatures and

---

<sup>2</sup>The “warm” and “cool” components have temperatures of typically 2.4–6 keV and  $\sim 1$  keV, respectively. Throughout this review we use these terms for these energy ranges, as well as  $kT > 7$  keV for “hot.”



emission measures of the second and third (“warm”) components may well be variable on timescales of weeks.

There is contradictory evidence of whether thermal components alone are altogether sufficient to describe the X-ray spectrum of “ $\gamma$  Cas stars.” In their recent study of  $\gamma$  Cas, [Shrader et al. \(2015\)](#), combined *Suzaku* and *INTEGRAL* data. This extended the energy range under study to 100 keV. These authors discovered that a thermal component having  $kT_{\text{hot}} \approx 14$  keV is adequate in their modeling to fit the data. The Shrader et al. fit to the continuum is shown in Figure 1 and supports this conclusion. However, in their studies of high resolution spectra of  $\gamma$  Cas, S04, L10, and S12 found the presence of relatively strong Ly  $\beta$ , Ne X and O VIII lines in the spectrum of  $\gamma$  Cas to be incompatible with a thermal model that fit the Fe XXV/Fe XXVI lines and surrounding continuum. At the high energy end of the spectrum the hinted existence of a relatively strong Fe XXVI Ly  $\beta$  line in the spectrum of the first known and brightest  $\gamma$  Cas analog HD 110432 was first noted on by [Torrejón & Orr \(2001\)](#) and discussed further by [Lopes de Oliveira et al. \(2007b, “L07b”\)](#). This feature is unresolved and merits modeling with improved description of the line formation mechanisms.

We remark also on the origin of the “cool” plasma component, which has an energy temperature  $kT_{\text{cool}} \approx 0.1$  keV. This value is roughly consistent with wind-shock plasma temperatures of other early B-type stars. However, the volume emission measure is a few times larger than shocks caused by B star winds (S04, L07b). This fact casts some doubt that we are observing the canonical B-star wind in this spectrum. Subsequent analyses by L10 and S12 of more recent *XMM* soft X-ray spectra has reinforced this doubt, for example because of their non-negative radial velocities and the short-term variations of only the soft X-ray flux. There is some ambiguity here because of the fact that the wind density varies as a function of latitude among Be stars. Also, the wind density for  $\gamma$  Cas has been known to vary with precessional phase of the disk-embedded density wave by about an order of magnitude ([Telting & Kaper, 1994](#)).

In our view the question of whether the fourth plasma component is due to the star’s wind is still open because we do not know whether the X-ray generation mechanism might influence the generation of winds.

To unpack the spectroscopic diagnostics revealed by each plasma component, we exhibit an “unfolded spectrum” of  $\gamma$  Cas as in Figure 2. The component spectra are computed with the XSPEC modeling program for an *XMM/RGS* observation on August 2, 2010 (S12). The observed spectrum is

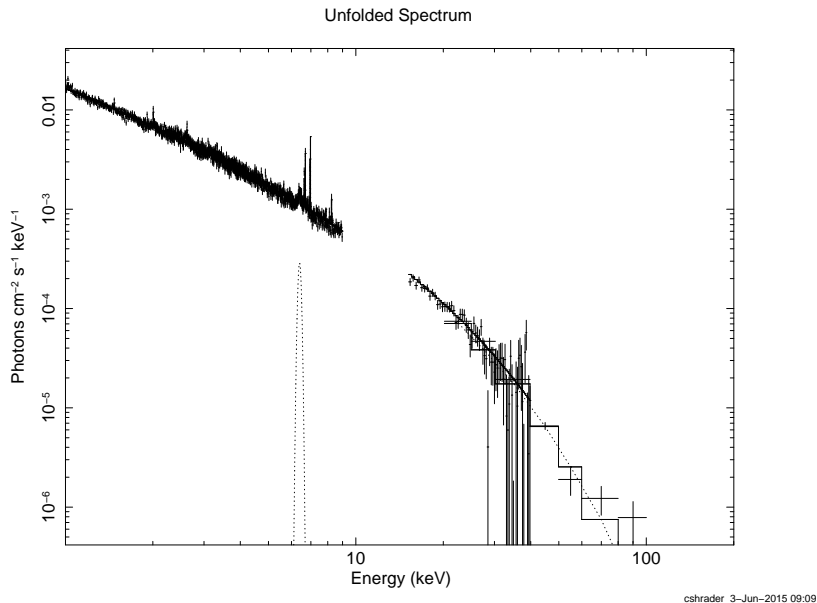


Figure 1: The high energy spectrum of  $\gamma$  Cas according to combined *Suzaku* and *INTEGRAL* observations. The fit is to an optically thin thermal model with  $kT = 14.4$  keV and a Gaussian to simulate the Fe K fluorescence feature. With permission of [Shrader et al. \(2015\)](#).

depicted by a dashed black line at the top. Note that the  $kT_{\text{hot}}$  component already almost matches the observed continuum spectrum, though not the line spectrum in the long wavelength range indicated. The figure clarifies how the emission line spectrum at longer wavelengths imposes the requirement that cooler plasmas be included in the overall spectrum model.

From these models one point should be stressed: *even at long wavelengths the flux of the hottest component dominates the continuum*. Then, for example, the attenuation of the soft X-ray flux is the sign of photoelectric absorption due to an intervening cold gas column along the line of sight to the hot site(s) situated in background.

## 2.2. Two absorption columns toward $\gamma$ Cas.

One of the fortuitous aspects of the modeling of these  $\gamma$  Cas data is the recognition that the broad range of continuum wavelengths allows one to determine that two separate absorption columns to the X-ray sources are required. The density for the first column,  $N_{\text{H}_a}$ , alone is consistent with the UV-derived ISM column. Thus, it is assumed to be nonlocal and unrelated

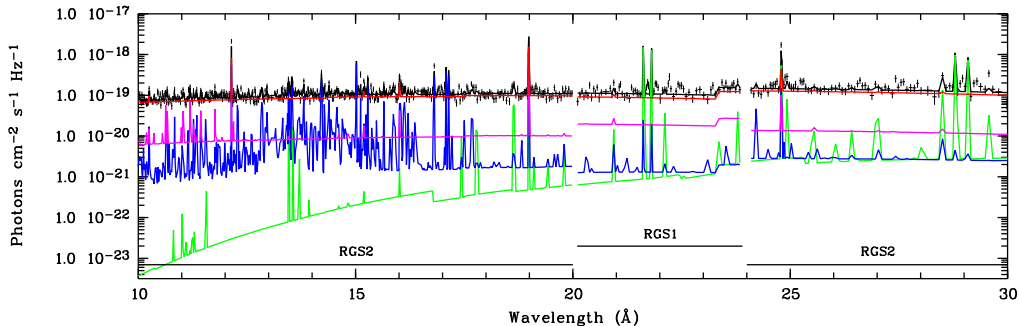


Figure 2: Line- or color-coded “unfolded” models for the *XMM/RGS* spectrum of  $\gamma$  Cas. Horizontal bars give the wavelength coverage of the separate RGS1 and RGS2 cameras. Sorted by temperature the components are shown as thin continuous ( $kT_{\text{hot}} = 12\text{--}14\text{ keV}$ ), thick continuous black ( $kT_{\text{warm},2} \sim 2.4\text{ keV}$ ), light dashed ( $kT_{\text{warm},1} \sim 0.64\text{ keV}$ ), and thick dashed lines ( $kT_{\text{cool}} \sim 0.1\text{ keV}$ ). In the on-line version the respective components are represented in red, magenta, blue, and green. After [Smith et al. \(2012\)](#).

to processes prevailing near the Be star. The additional column,  $N_{\text{H}_b}$ , affects only the hot plasma component, at least so far as current quality X-ray spectra allow us to know. It exceeds the ISM value typically by a large, time-variable factor ( $2\text{--}740\times$ ), but it covers only one quarter of the hot plasma site(s), a fraction that S04 expected based on the assumption that the emission sites are distributed randomly across and close to the Be star’s surface and also on the inclination of  $\gamma$  Cas to our line of sight;  $\frac{1}{4}$  is the ratio of the visible areas in the star’s “Northern” and “Southern” hemispheres. The upper part of Figure 3 depicts for  $\gamma$  Cas the effects of attenuation on the soft X-ray region due to the ISM ( $N_{\text{H}_a}$ ) and  $N_{\text{H}_b}$  columns (i.e., as observed), and also flux corrected as if only the  $N_{\text{H}_b}$  column were present. Additionally, it shows the correction to the flux as if neither column were present. The lower part of the figure highlights the effect for the  $\gamma$  Cas analog HD 110432 with the single absorption column,  $N_{\text{H}_a}$ , present (as observed) and also corrected for the effects of this absorption. Thus, the highest two flux spectra in this figure (spectra *b* and *e*) represent what the spectra would look like without any intervening absorption.

### 2.3. Spectroscopic measures of the volumetric density.

The density-sensitive *rif* (resonance/intercombinational/forbidden) triplet lines are widely used in X-ray spectroscopy to estimate the volumetric den-

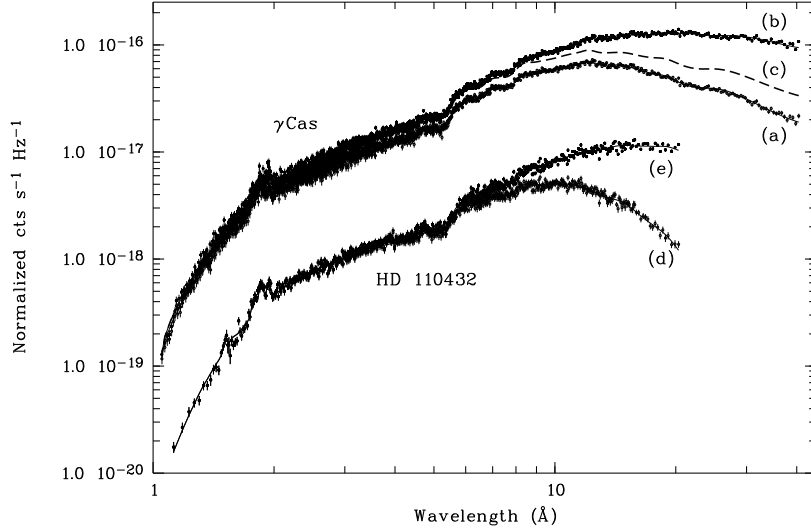


Figure 3: *XMM* spectra of  $\gamma$  Cas (spectra (a-c) and HD 110432 spectra (d-e)). Spectra (a) and (d) are the observed spectra on August 24, 2010 and July 3, 2004 for the respective sources. The remaining three are pseudo-spectra representing the observed spectra corrected for the modeled local ( $N_{\text{H}_b}$ ) and/or ISM ( $N_{\text{H}_a}$ ) absorption column. Spectrum (b) shows the effect of removing both local and ISM absorptions toward  $\gamma$  Cas, whereas spectrum (c) depicts the spectrum as if only the ISM absorption were removed. Spectrum (e) represents the removal of the single-column absorption toward HD 110432 due to the ISM.

sity of a hot emitting plasma. For the  $\gamma$  Cas spectrum the absence of the forbidden component and the near equality of the  $r$  and  $i$  line components arising from He-like ions Si XIII and Ne IX could itself indicate a high density ( $\gtrsim 10^{11} \text{ cm}^{-3}$ ) for the “warm” plasma components. However, the implied dominance of collisions setting these ratios could just as easily be caused by quenching due to collisional deexcitation due to far-UV radiation from the nearby Be star. Therefore, the triplets turn out not to be decisive indicators of the local plasma densities. Nonetheless, S12 pointed out that the observed ratios of certain L-shell Fe ion lines is consistent with even higher densities ( $10^{13}$ – $10^{14} \text{ cm}^{-3}$ ) for the “warm” components, according to the models of [Mauche, Liedahl & Fournier \(2001\)](#). The typical density of the  $kT_{\text{hot}}$  plasma is at least this high (see §3.1).

Table 1: Density column (units of  $10^{22} \text{ cm}^{-2}$ ), EW (mÅ) of Fe fluorescence, Abundances.

Date	$n_{\text{H}_b}$	EW(FeK $\alpha$ )	Fe	Ne	N
2001	10	-19	0.10	$\sim 1$	$\sim 1$
2004	0.023	-10	0.12	2.63	3.96
2010	36-74	-35 to -50	0.18	1.80	2.33

*Notes:* (1) Errors for [Fe $_K$ ], [N], and [Ne]:  $\pm 0.02$ ,  $\pm 0.75$ , and  $\pm 0.28$ , resp.; solar units. (2) 2010 abundances are 4-epoch averages. (3) All spectra analyzed are from the *XMM* except the *Chandra* spectrum in 2001. (4) After [Smith et al. \(2012\)](#).

#### 2.4. Correlations with the $N_{\text{H}_b}$ column.

A surprise from these analyses was that the strengths of several important spectral lines and their possible correlations with the  $N_{\text{H}_b}$  column are evident over time. Of particular note, varying line strengths are those for which Fe, Ne, and N abundances are derived, and these often lead to nonsolar abundances. In particular, the lines are those from the K-shell ions only of Fe XXV and Fe XXVI and the Ne and N abundances from Ly $\alpha$  lines of Ne X and Ne IX and N VII and N VI ions. In contrast to the Fe abundance derived from the L-shell ion lines, which is solar-like, the equivalent widths of Fe XXV and Fe XXVI lines are abnormally weak, indicating a low abundance - see Table 1. This particular anomaly was first noticed in the first moderate resolution *Tenma* spectrum (M86), and to varying degrees it has betrayed itself in every short wavelength spectrum of  $\gamma$  Cas published since.

#### 2.5. The FeK fluorescence feature.

In addition to the emission lines noted, the  $\gamma$  Cas spectrum shows the well known “FeK $\alpha$ ” fluorescence feature centered near 1.93 Å. This blended feature is produced by irradiation of hard ( $\gtrsim 8$  keV) continuum X-rays and the resulting fluorescence  $\alpha$  transition from any of several low to intermediate ions of Fe in “cold” circumstellar gas or by scattering of X-rays from the surface of a nearby hot star. The feature is typically modeled as an *ad hoc* Gaussian from which its equivalent width (EW) is determined. The precise centroid wavelength ( $1.931 \pm 0.006$  Å) S12 measured for the fluorescent feature is consistent with radiative interactions with Fe I-Fe XVIII ions. This is also the basis for our referring to the fluorescing agent as “cold” gas.

[Giménez-García et al. \(2015, “G15”\)](#) have provided an important clue to the nature of the environment of X-ray emitting plasma in  $\gamma$  Cas stars. These authors compared the strengths of FeK $\alpha$  and recombination lines of

Lyman  $\alpha$  FeXXV and FeXXVI for High Mass X-ray B (HMXB) stars at large and  $\gamma$  Cas analogs in particular. The latter differ from the former in two important respects. First, only the well investigated  $\gamma$  Cas analogs exhibit visible fluorescence and recombination Fe lines – see also [Lopes de Oliveira \(2007a, “L07a”\)](#). Second, the  $\gamma$  Cas stars do not share the HMXB property of exhibiting an inverse correlation between EW(FeK $\alpha$ ), that is of the FeXXV and FeXXVI lines and X-ray luminosity. Thus, the behavior of FeK $\alpha$  sets the two groups apart: the spectra of the best known  $\gamma$  Cas stars are unique among high mass X-ray stars by exhibiting visible FeK $\alpha$  and FeXXV and FeXXVI recombination lines. This behavior suggests that new analogs can be potentially discovered among known Be stars by spectra over a narrow energy range, at least if the instrumental detection ability at these energies is sufficient. In case of a photon dearth the hardness of the continuum combined with the presence of an unresolved FeK line tells us that dedicated follow-up X-ray observations should be undertaken to clarify the results of a faint-source survey.

It will be important to confirm these trends with continued observations. Here we note that the apparent correlation of the strength of the FeK fluorescence feature with  $N_{\text{Hb}}$  (Table 1) strengthens the case that the feature is created from emission of hard X-ray continuum photons into the line of sight from nearby cold matter. The abundance results present a puzzle, even though a possible way out is that it represents an IFIP (Inverse First Ionization Potential) effect. IFIP/FIP effects are probably somehow caused by a selective diffusion of ions across a magnetic plasma ([Güdel & Nazé, 2009](#); [Laming, 2004a,b](#)). The efficacy of this diffusion depends on the potentials of their first ionization stages.

### 3. X-ray flux and related optical/UV variations

In §1.2 we stated that the X-ray flux of  $\gamma$  Cas varies on four basic timescales. We discuss them in order of length of these timescales. Because many of these variations have been well explored for HD 110432, the brightest  $\gamma$  Cas analog, we place the discussion of the light curves of this star in this section as well.

#### 3.1. X-ray “flares.”

Starting with studies of the  $\gamma$  Cas X-ray light curve, [Parmar et al. \(1993\)](#) – *Exosat*) and [Horaguchi et al. \(1994\)](#) – *Ginga*), it became clear that “shots”

or flare-like events are present in all light curves.<sup>3</sup> They were found to be statistically robust and therefore astrophysical in origin and also to exhibit  $1/f$ -like power spectra.

### 3.1.1. Light curves and power spectra.

The first discovery of a single strong flares in the  $\gamma$ Cas light curve was discussed by M86 from a *Tenma* light curve. This instrument was sensitive to the energy range 1.3-10 keV. Observations by the *RXTE*, early in its mission when its *PCA* detectors were optimally efficient, succeeded in pushing the short duration (FWHM) limit to 4 seconds (SRC98), where the limit still is today. An *XMM/EPIC* light curve, covering the energy range 0.3–10 keV and shown in Figure 4, is instructive in the characteristics it shows. First, we can see the presence of a background or “basal” envelope, which actually constitutes between 60% and 70% of the total flux measured by *RXTE* within the 2–12 keV range. This slowly varying envelope is punctuated by distinct “flares,” whose amplitudes range from barely detectable to twice again the local basal flux. In general these weak flares are far more numerous than the strong ones and comprise most of the X-ray flux attributable to flares (RSH98, RS00, [Smith, Lopes de Oliveira & Motch \(2012, “SLM12”\)](#)). Individual flares overlap typically  $\frac{1}{4}$  of the time, thereby giving the impression in low quality time series that they can last as long as a few minutes - these are (at best) semi-resolved “flare aggregates.”

Since these two flux components are roughly equal, they both contribute important details to a power spectrum of X-ray emission. Figure 5 represents the power spectra of two observations of  $\gamma$ Cas two years apart. In these observations the astrophysical signal can be seen rising from white noise at high frequencies to greater values at lower frequencies. The spectrum is almost linear in a log-log plot. A sharp eye may notice that the typical slope is not quite -1 in the frequency range  $10^{-3}$ – $10^{-1}$  Hz, as one expects from “flicker”  $1/f$  noise. It is more correctly described as “pink noise,” which refers to a nonequilibrium-driven dynamical system. The plot shows that variations on timescales of several hours dominate and these will be taken up in the next section. RS00 discovered that details in the power spectrum,

---

<sup>3</sup>We loosely defined a flare as a sudden, short-lived increase in X-ray flux. The term does not necessarily connote a localized explosive magnetic instability, as on the Sun.

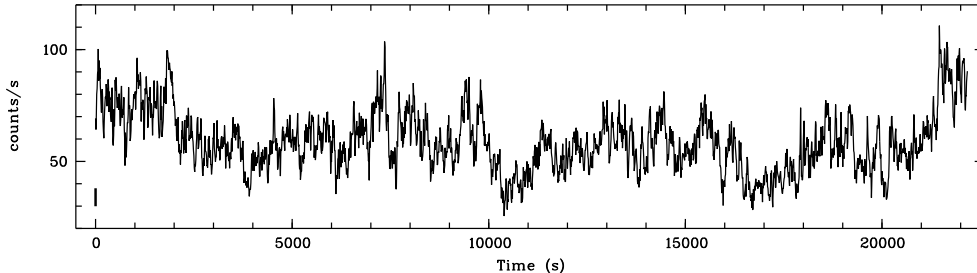


Figure 4: A stretch of the *XMM/EPIC* light curve of  $\gamma$  Cas on 2004 February 5. The indicated flux error is a typical value determined by the data reduction pipeline, in this case for 10s binning. The data show both flares and an underlying basal flux envelope.

including the mean slope in the range referred to above, are sensitive both to changes in the distribution of flare strengths and the relative importance of slow changes in the basal flux (see §3.3). These factors also contribute to the prominence of a slight break in the power spectrum slope at 0.003–0.005 Hz. In particular, a break can occur if there are *relatively* more strong and long-lived flares (or chance unresolved aggregates) than at other epochs.

### 3.1.2. Attributes of individual flares ( $\gamma$ Cas and HD 110432).

Several attributes of the resolved flares have been determined for  $\gamma$  Cas and HD 110432. First, in a statistical analysis of a number of short-lived flares with high-quality *RXTE* light curves, SRC98 found that their profiles are symmetrical, suggesting that their decay times are shorter than the detectable FWHM lifetime limit of 4 s.

Second, the number distributions of flare energies over two different epochs have been found to follow exponential functions (RS00, SLM12), rather than a power law, as for solar magnetic flares (RS00; SLM12). This is true for flares observed in HD 110432. On the other hand, SLM12 point out that a power law distribution could *appear* log-linear if the range of flare energies sampled is truncated by instrumental constraints, as is the case for our sources.

Third, the upper limit to resolved flare lifetimes is about 150 s for  $\gamma$  Cas and about 100 s for HD 110432. Most flare lifetimes lie well within low and high limits, namely 10–30 s. Mean flare lifetimes and energies can be different at different times (SLM12).

Fourth, a comparison of the flare rates of  $\gamma$  Cas and HD 110432 - using both *RXTE/PCA* and *XMM* data showed that once account is taken of HD 110432



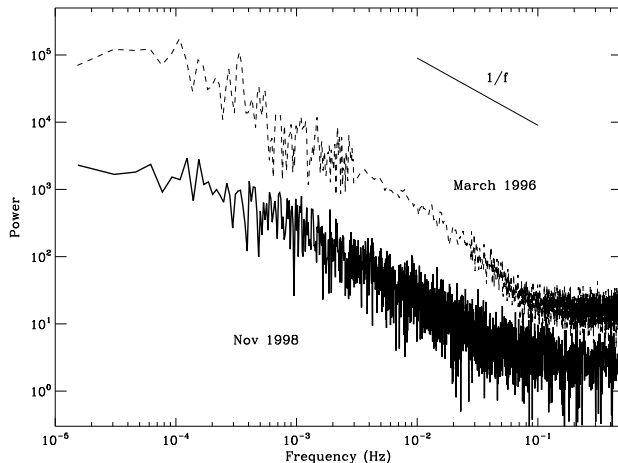


Figure 5: Power spectrum of March, 1996 and November, 1998 *RXTE* observations (binned to 4s). Photon (white) noise is shown in the lower right. The logarithmic slopes between frequencies  $10^{-3}$  Hz and  $3 \times 10^{-2}$  Hz are  $-1.36 \pm 0.10$  Hz and  $-1.23 \pm 0.13$  Hz, respectively, i.e., nearly identical but marginally statistically different from -1. After [Robinson & Smith \(2000\)](#).

being 11 times fainter in the 0.2–12 keV X-ray band than  $\gamma$  Cas, the flare rates of the two stars are equal to well within measurement errors (SLM12). This rate is 0.009–0.012 flares $^{-1}$ . According to studies of flare rates at different epochs, the variance within this range is caused mainly by actual changes in the flare rate with time.

Fifth, SLM12 studied the interval of time between successive flares and found the distribution was consistent with their occurring randomly.

Statistically, X-ray colors of flares are typically rather close to colors of neighboring basal flux. For  $\gamma$  Cas and HD 110432 small inequalities of colors do sometimes occur and with either sign. Generally, the  $\gamma$  Cas flares tend to be systematically softer or harder than the basal flux for hours or more at a time (RS00). However, it is occasionally the case, particularly for HD 110432, that flare to basal colors can reverse in even several minutes, according to SLM12. These authors found that 75% of the time the flare strengths are comparable in soft and hard X-ray bands. For 15–20% of events in their study soft X-ray flares were stronger than their hard counterparts, while in the remaining 5–10% of the cases the reverse was true. These studies demonstrate in the main that the flare-producing energy reservoirs are fairly constant in terms of their mean injected energy, though they can at times

vary dramatically.

### *3.1.3. Differences between flares in $\gamma$ Cas stars and the Sun.*

Since we know a great deal about the release of X-rays from magnetic activity on the Sun, it is worthwhile comparing the phenomenology of solar flares with what we observe in the rapid X-ray events in  $\gamma$  Cas. Actually, a comparison of true solar flares with flare-like events in the light curves of  $\gamma$  Cas and HD 110432 show more differences than similarities. An energetic flare on  $\gamma$  Cas can be up to  $10^{33}$  erg s<sup>-1</sup>, which is orders of magnitude more than an energetic solar flare (although in rare cases solar flares have been observed releasing this energy). Flares on the Sun or active lower main sequence stars may last many minutes and exhibit slowly decaying tails. Solar flares tend to show a power law distribution. As noted, while the  $\gamma$  Cas flare number distributions seem to show a different law than solar flares, it could be illusory. Even so, studies of  $\gamma$  Cas flaring distributions over time indicate that their slopes vary, and this is not a data sampling artifact. Nor is it a characteristic of typical solar flare distributions.

Another difference with flares in small active regions on the Sun is that flares in  $\gamma$  Cas are typically well spaced in time from one another [Smith, Lopes de Oliveira & Motch \(2015, “SLM16”\)](#)). They do not occur as on the Sun and active cool stars in clusters or cascades ([Aschwanden, 2011](#)). Flare cascades are a result of “Self Organized Criticality,” an unstable condition which can trigger multiple flares locally. In contrast, flares on  $\gamma$  Cas and HD 110432 give every indication of being triggered independently of one another (SLM12). This seems to be a fundamental difference from true flares on the Sun and related active cool stars. Also, SRC98 pointed out that the presence of flares is correlated with the introduction of matter (co-rotating clouds) over areas over the surface.

### *3.1.4. Determining physical gas properties from flare attributes.*

In the first statistical analysis of flare properties of  $\gamma$  Cas, SRC98 found a strong correlation between the flare (upper) and basal (background) flux envelopes as the X-ray light curves varied over timescales of an hour or longer. This result, the observation that the basal and flare colors are usually almost indistinguishable from one another, all combined with the argument that the creation of basal flux *results* from the flares imply that the flare energy decays adiabatically (SRC98). That is, the flare duration is essentially set

by the flare parcel expansion time and not the cooling timescale. Applying these inferences, and the fact that the X-ray emission is optically thin, SRC98 showed that the exploding flare parcels are typically small (radius  $\sim 5000$  km). Also, *they arise in plasma densities of  $\gtrsim 10^{14}$  cm $^{-3}$* . This last conclusion arises mainly from the observed lifetimes of the most short-lived flares and is therefore venue-independent: the density and volume estimates derived for the hot plasma sites pertain to whatever the physical mechanism for X-ray generation. This argument reinforces, though is much stronger than, results from spectroscopic diagnostics of density discussed in §2.3.

### 3.1.5. Implications for the generation of hard basal flux.

SRC98 investigated the creation of basal X-ray flux for  $\gamma$  Cas as a follow-up to their examination of plasma cooling properties of X-ray flares. They found that after an initial injection of high energy, gas parcels with typical sizes of a few thousand kilometers, expand explosively on a timescale of 5 s. Typically some 4% of their energy is lost during this adiabatic phase. Eventually radiative cooling dominates the expansion, but only after further expansion is halted by overpressure from an external mechanism. In view of the presumed role of magnetic fields in enforcing corotation of UV-observed clouds, SRC98 attributed the confinement to the anchoring of field line loops emanating from the Be star's surface.

During the post-flare cooling stage one should expect to detect emission from a continuum of temperatures if the gas expansion continues unabated. L10 and S12 tested the idea of *in situ* cooling by searching for the presence of a DEM, that is by plasma emission over a continuous range of temperatures instead of one or more discrete ones. Their work showed that the DEM description did not result in a model that gave an acceptable fit to the X-ray emission line spectrum and thus argued against a continuous and unconstrained plasma cooling.

In their discussion of the generation of basal flux, SRC98 adopted a characteristic volumetric density of  $10^{11}$  cm $^{-3}$  based on the timescale of changes in the basal flux and also the frequency where the power spectrum tends to depart from a linear  $1/f$  relation (Figure 5). Using this value and using flare-canopy plasma models developed for solar flare regions, these authors found that an individual flare expands into a canopy with projected area of  $\sim 0.002$  of the star's and a height of  $\sim 0.05R_*$  above the star's surface. These numbers are self-consistent in the sense that they predict the generation of

the observed X-ray emission measure of  $\sim 3 \times 10^{55} \text{ cm}^{-3}$ . They also assume that at any moment we observe a total of 10–20 flare and basal emitting regions. SRC98 estimated the mean magnetic fields within these confined regions to be  $\sim 200$  gauss. We stress that these estimates ultimately hinge on the assumption that the immediate post-flare expansion is abruptly braked within a magnetically confined volume. The result is that the basal and flare temperatures are about equal. In §6.2.1 we will discuss initial conditions that might lead to the creation of surface flares.

### 3.2. Where do the warm plasmas reside?

The least understood of the X-ray emitting components in  $\gamma$  Cas and HD 110432 are the one or two so-called warm plasmas (defined again with  $kT_{\text{hot}} \approx 2.5\text{--}6 \text{ keV}$ ). This is because these components are visible mainly through their line spectra; their continuum emission can be interpreted only roughly through an X-ray colors defined across short and long wavelength subdomains. A few studies (Smith, Robinson & Corbet, 1998; Lopes de Oliveira et al., 2007b; Robinson & Smith, 2000) comparing rapid time series behavior between soft and hard X-ray light curves indicate that they often do not coincide, and this has been taken as evidence that the warm plasmas are not copatial with the hard X-ray sites. As noted in §2.3, the *rif* ratios arising from He-like ions do not advance the issue. The observation of certain FeL lines noted in the same previous discussion could lead to densities as low as  $10^{13} \text{ cm}^{-3}$ . This is consistent with the base density of the disk.

Another interesting diagnostic is the local turbulent velocity measured from the (symmetric) lines arising from the warm plasma. This broadening is of the order of  $500 \text{ km s}^{-1}$  (Smith et al., 2004, 2012), although in one case, possibly an outlier, a value as high as  $950 \text{ km s}^{-1}$  was reported. The salient point here is that velocities derived from warm plasma lines are inconsistent with the higher values of thermal broadening of the hot plasma ( $\gtrsim 1500 \text{ km s}^{-1}$ ; SRC98).

In addition, in their *HST/GHRS* time series spectra SR99 found no correlation between the presence of hot plasma lines of Fe V shifted by the same velocities at which Si III 1417 Å (a warm plasma line) features were found.

These discoveries validate the conclusion from the X-ray color curves noted just above that the warm plasmas are emitted in another place – even if their formations are associated (that is, generally correlated) with one another.

S04 speculated that the warm plasma could be created either by collisions of hot plasma, or perhaps by an initial accelerated electron beam, into disk material or as an attribute of the slowing of the plasma cooling as the losses move through plateauing cooling curves due to certain dominant metallic ions in the plasma. However, the improved accuracy of the component determinations in the [Smith et al. \(2012\)](#) study also indicates the absence of plasma emission between the emitting components. This suggests to us by now that the continuously cooling scenario is a less likely explanation.

As for the companion cool ( $kT_{\text{cool}}$ ) plasma component, in addition to the arguments mentioned in §2.1 one should emphasize the fact that this component shows lines leading to solar (at least for [C]) abundances indicates that the soft spectrum is formed in an optically thin plasma.

In general, it must be said that the location of the warm and cool plasmas and their role in local energetics near the Be star are not yet understood. The high throughput of the envisaged Athena X-ray satellite, and in particular the high spectral resolution capabilities of its planned X-IFU instrument, will allow exquisite time-resolved spectroscopy. Line ratios, profiles and velocities will provide key diagnostics on the location and properties of the hot, warm and soft thin thermal emitting regions.

In addition, future observations with a larger aperture X-ray telescope can tell us whether the emission lines emitted by the warm plasma are attenuated or not by the  $N_{H_b}$  column, which so far is defined mainly for the hot plasma sites in the  $\gamma$  Cas spectrum. If  $N_{H_b}$  affects the warm sites too they are probably be located near the hot sites, even if they are not cospatial with them.

### 3.3. Quasi-random undulations of the X-ray and UV light curves.

Using the then novel capabilities of the *RXTE/PCA* and *ASCA* detectors, SRC98 and [Kubo et al. \(1998, “K98”\)](#), respectively, highlighted quasi-random undulations in the X-ray light curve of  $\gamma$  Cas on timescales of 2–3 hours. Examples of these variations are exhibited in Figure 6 and are responsible for much of the X-ray power at frequencies  $\lesssim 10^{-3}$  Hz. These particular *RXTE* observations were unique in that they were executed simultaneously with the Goddard High Resolution Spectrograph (GHRS) aboard the *Hubble Space Telescope* on a 21 hour campaign in 1996 (hereafter the “1996 campaign”). The GHRS spectra were centered on the Si IV line multiplet at  $\lambda 1394$  and  $\lambda 1403$ . These spectra were binned to 60 s. Next the fluxes were coadded over a stretch of quasi-continuum wavelengths to form a UV light curve ([Smith,](#)

Robinson & Hatzes, 1998). This light curve showed a series of striking correlations or anticorrelations with the X-ray variations during this duration. One of these relations was the anticorrelation of the *RXTE* fluxes and the UV light curve. The latter showed dips of 1–2% depth corresponding to X-ray maxima. These maxima were accompanied by increases in the basal flux. This suggested that the increased X-ray flux is associated with intervening structures that absorb UV light from the Be star’s surface.

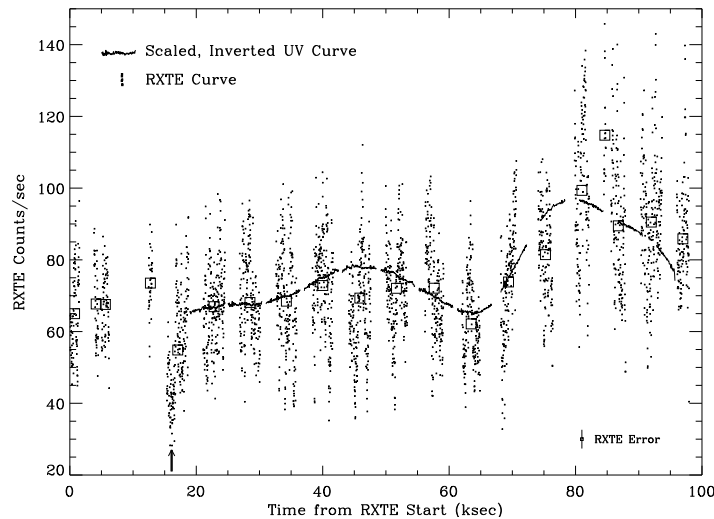


Figure 6: Simultaneous *RXTE* light and HST/GHRS light curves of  $\gamma$  Cas obtained on March 14–15, 1996. GHRS spectra have been binned in wavelength to form a “UV continuum” light curve. The latter curve has been inverted and scaled to match variations in the *RXTE* light curve. The X-ray variations are emphasized by orbital averages (open squares). The X-ray data are binned to 16 s; their high frequency “noise” is due to flaring. The upward arrow in the lower left exemplifies an X-ray “cessation” (see text). After Smith, Robinson & Corbet (1998).

RSH02 first attempted to model the UV continuum dips by supposing that they were caused by rotationally advected black spots across the Be star’s surface but were unable to do so. The problem was that the variations are too short-lived to match the durations of these features. These authors were able to match the light curves with elevated translucent “clouds” forced into corotation above the star. The typical sizes and elevations of these structures was found to be  $0.2\text{--}0.3R_*$ , on the assumption of forced corotation and that the blobs cross move parallel to the equatorial plane. The determined elevation of these clouds allows the transits to be brief enough to match the duration

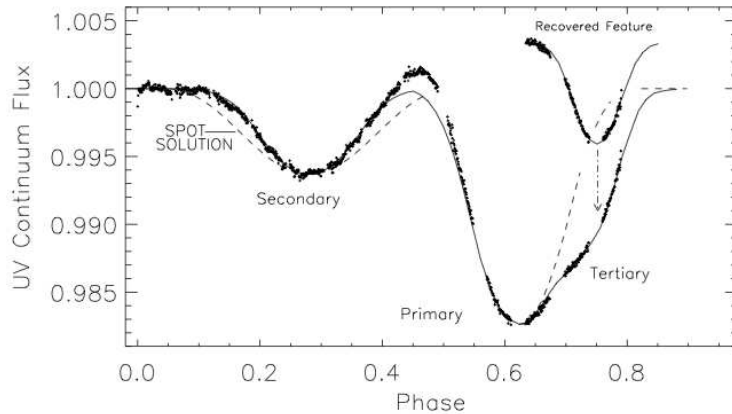


Figure 7: The March 14-15, 1996 UV continuum light curve of  $\gamma$  Cas. This is fit with models of a rotationally advected surface spot (dashed line) and three clouds forced into corotation with radii of  $\approx 0.3R_*$  and elevated by a similar distance above the star’s surface (solid line). The dashed line is the closest fit possible for the spot model and is still inadmissible. After [Robinson & Smith \(2000\)](#).

of the light curve dips. Figure 7 exhibits the best fits to a single advected surface spot (unsuccessfully) and successfully to three elevated clouds.

In addition to the March, 1996 *HST/RXTE* campaign, [Smith & Robinson \(1999, “SR99”\)](#) also undertook a 33 hour-long (with short interruptions) high-resolution *IUE* campaign on  $\gamma$  Cas in January 1996. They again constructed light curves of mean fluxes in each echelle order and found features in the time series they identified as similar dips to those found in the *GHR*S time series. They discovered that the observed dip minima grew monotonically stronger with decreasing wavelength, that is across the *IUE* echelle orders. Applying blanketed model atmosphere spectral syntheses, they were able to show that this progression with wavelength could be explained by translucent clouds with a temperature of  $\lesssim 10$  kK, which is very different from the temperature expected in low density gas occupying the outer fringes of the Be star photosphere. Note that although this temperature is in the expected range of matter in intermediate or outer regions of the Be disk, we do not believe the dips originate from matter in the disk. The disk matter rotates around the star at a Keplerian rate, or at  $\approx 1R_*$  nearly so. Therefore any putative stable blobs constrained in the disk itself would transit the stellar disk *too slowly* to be consistent with the dips in Figure 7. We note in passing that given these trends with wavelength from *IUE* spectra, it is not surprising

that corresponding dips have not been discovered in the optical light curves of  $\gamma$  Cas, as noted by [Smith, Henry & Vishniac \(2006, “SHV06”\)](#).

#### 3.4. Migrating subfeatures line profiles of $\gamma$ Cas and HD 110432.

[Yang, Ninkov & Walker \(1988\)](#) discovered the presence of “migrating subfeatures,” or *msf*, in spectral lines of the optical spectrum of  $\gamma$  Cas.” These appear in the grayscale of timeseries of spectra. These are narrow absorptions moving steadily from the blue to the red edge of a rotationally broadened line profile, often to be followed several hours later by a new *msf*. The existence of *msf* was initially discovered in an unrelated type of star, a magnetically active young K5 V star known as AB Dor ([Cameron-Collier & Robinson, 1989](#)).

*Msf* cannot arise from rotationally-advected black spots, as on the Sun, for several reasons. For example, their motion across the line profiles would indicate, as for the UV-absorbing larger “clouds” discussed above, super-critical stellar rotation. The features occur perhaps at irregular intervals during some nights of observation and sometimes not at all ([Smith, 1995](#)). Because of their erratic appearances and their narrow subprofiles compared to the intervals between them, they are not consistent with the more smoothly varying (and generally evenly spaced) “wiggles” in line profiles that are characteristic of surface nonradial pulsations in other B stars. The *HST/GHRS* campaign in March, 1996 that we have noted included weak lines located near the Si IV doublet at 1394 Å and 1403 Å. SRH98 constructed a grayscale time series of 1280 spectra, each binned over 1 minute. Figure 8 exhibits a portion of their grayscale in the range 1404–1417 Å (where few effects from variations of the nearby Si IV resonance lines occur).

Dominating this figure is a pattern of diagonal striations running from the lower left (short wavelengths, starting spectra) to upper right. Their mean acceleration is  $+95 \text{ km s}^{-2}$ , close to values found for *msf* in optical spectra of  $\gamma$  Cas ([Smith, 1995](#)). These features were found by [Yang, Ninkov & Walker \(1988\)](#) and [Smith \(1995\)](#) in optical lines of the  $\gamma$  Cas spectrum with very nearly the same acceleration rates. This fact suggests that, similar to the UV continuum dips discussed above, these features arise from cloudlets, that are forced into corotation a few tenths of a stellar radius (at most) above the Be star’s surface. The inference that they are elevated comes largely from the fact that their acceleration rate is slightly too fast to be due to surface advection of spots. The *msf* striations in our figure can be shown to arise



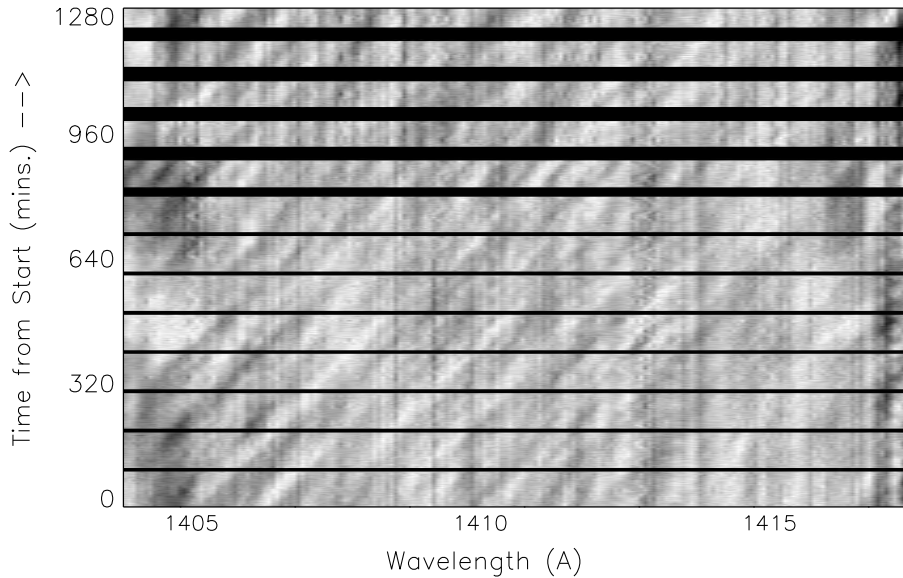


Figure 8: The 1404-1416.5 Å spectrum of  $\gamma$  Cas during the 1996 HST/GHRS campaign, which consists of 1280 spectra each binned over a minute. The dark diagonal striations moving upward and to the right are the *migrating subfeatures* in the spectrum of many faint spectral lines. These *msf* arise from the Doppler imaging of small translucent clouds in the foreground. Individual features last no longer than one to a few hours (2 orbital segments of the time series). The limits of a rotationally broadened line profile at these wavelengths is about two Ångströms. The rate of migration of these features across the underlying line profiles is best explained by their forced corotation over the star’s surface. Modified from [Smith, Robinson & Hatzes \(1998\)](#).

from  $\sim 10$  spectral lines identified from Fig. 4b of SR99 and thus their local velocities are known.

A close inspection of Figure 8 discloses that the strengths of these *msf* are quite variable. In fact, no individual *msf* lasts for longer than one to a few hours, which suggests an environment in which small cloudlets are constantly forming and quickly disappearing.<sup>4</sup> It may or may not be coincidental that

---

<sup>4</sup>The rationale for calling the structures responsible for *msf small*, as opposed to the larger clouds responsible for dips in UV light curves, is twofold: (1) their existence is more ephemeral (small structures can more easily dissipate) and (2) a structure of a given size, having properties distinguishing it from the background photosphere, is generally much more visible in a spectrum than the continuum.

the timescales for the changes of *msf* strengths and basal flux are the same,  $\sim 1000$  s. It should be noted that this type of ephemeral behavior is not generally descriptive of the circumstellar environment of other Be stars – nor does it describe the behavior of matter in the inner parts of their decretion disks.

It is important to add that [Smith & Balona \(2006, “SB06”\)](#) published time series spectra of the He I 6678 Å line HD 110432 that also showed likely *msf* on two of six ground-based observing nights. To sum up, *msf* have been reasonably well documented in spectra of only three stars: the object in which they were discovered (AB Dor),  $\gamma$  Cas, and the  $\gamma$  Cas analog HD 110432. Serial high-resolution spectra have not yet been observed in other analogs to see if they are a universal property of the class.

One may contrast the *msf* with the appearance of moving bumps in spectral absorption line profiles of unrelated Bp or Be stars. These features arise from a vectorial sum of local projected rotational and nonradially pulsational (NRP) velocities in a star’s photosphere. Bumps from nonradial pulsations are common in line profiles of Be stars and, except for interferences among comparable amplitude modes, occur regularly. (Thus, even if bump amplitudes transit the line profiles irregularly the quasi-periodicity of the NRP disturbance is evident in periodograms of light curves.) In addition, whenever these NRP features are visible in line profiles they represent surface waves generally traveling across the visible hemisphere. Line profile bumps are also often present (sometimes as emission as well as absorption features) in spectra of magnetic Bp stars, corresponding to accumulated matter in the two intersections of the magnetic and rotational equators. Such features also appear at regular intervals. Both of these examples are phenomenologically distinct from the *msf* in  $\gamma$  Cas, a fact that stems from their formation in different locations relative to the star’s surface.

One unique report by [Hanuschik & Vrancken \(1996\)](#) is of moving “narrow optical absorption components” (NOAC) through optical line profiles of spectra of 48 Lib (B3IV e-sh). Although these features exhibit a few similarities with the *msf*, they also have important dissimilarities. The latter include: (1) the NOAC are present only in low excitation metallic lines (generally recognized as “shell” lines), (2) their spectral widths are consistent with only thermal broadening, and (3) they occur only within a narrow radial velocity range of line center. Like the authors themselves, we do not know the physical origin of the NOAC features, other than they clearly are formed in orbiting shell clumps orbiting 10’s of radii from the star. Nonetheless, the

phenomenological *dissimilarities* argue that the NOAC have a different origin from the *msf*. It would be edifying to find them in the spectra of any other Be shell star,  $\gamma$  Cas analog or otherwise.

### 3.5. Further intermediate X-ray/UV correlations in the 1996 campaign.

In addition to the correlation between X-ray and *GHR*S-observed UV continuum fluxes observed of  $\gamma$  Cas in 1996 (Figure 6), various UV line strengths were found to be associated with the X-ray variations. Some of these are documented in Figure 9. *This figure shows that when the X-ray flux increases the strengths of Fe V absorption lines weaken (hence their fluxes increase), whereas at the same time the Si III and Si IV lines strengthen.* SR99 found that Si III–SiIV and Fe V lines are expected to be formed in matter located just above the surface of a B0.5 star.<sup>5</sup> The parameters of circumstellar gas are such that irradiation by nearby X-rays is either increased or decreased, respectively.

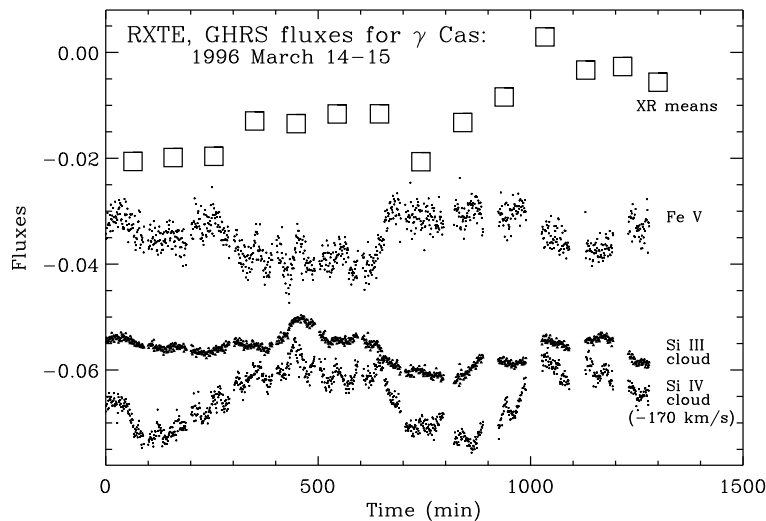


Figure 9: Variations of UV line fluxes against X-ray fluxes during the *GHR*S and X-ray campaign in March 1996. The ordinate for the UV lines is expressed in units of the local continuum flux. The rescaled X-ray flux averages (open squares) are taken from Figure 6 and reflect a change of a factor of 2. After [Smith & Robinson \(2003\)](#).

<sup>5</sup>The spectral line synthesis models suggest that Fe V lines are formed in an ambient gas with temperature of  $34\text{--}45\pm 3\text{ kK}$ . This is higher than the  $T_{\text{eff}} \sim 28\text{ kK}$  for  $\gamma$  Cas.

SR99 discovered correlations of X-ray flux with other UV line diagnostics in their 1996 *GHR*S observations as well. For example, the 1412.9 Å line, attributed to the underionized stage Fe<sup>+</sup>, exhibited a similar anticorrelation, as did the SIV 1404.7 Å line and several other features arising from less excited ions.

Surprisingly, and unlike most neighboring weak lines, the nearby UV resonance Si IV lines exhibited no internal migration patterns at all, even though SR99 were able to simulate this behavior in a nearby SIV line. The authors explained this unexpected behavior by the addition of a separate optically thin column to their spectral line synthesis model. Thus, their modeling of these UV lines indicated the presence of *two* columns: while most of the lines of sight were optically thick in the center of the spectral line, it is required that a smaller number of sight lines be optically thin.

### 3.6. Claimed periodicities on timescales of hours.

Early in the exploration of the X-ray properties of  $\gamma$  Cas, astronomers searched for periods in the expectation that robust X-ray pulsing would be observed that would clearly indicate that  $\gamma$  Cas is a magnetized rotating Be-pulsar or perhaps a highly magnetized Be-WD system. However, these hopes have not been realized. Frontera et al. (1987) reported the existence of “pulses” with a period of about 6 ks based on the observation of four equally spaced maxima in the *EXOSAT* light curve. Parmar et al. (1993) reexamined the Frontera et al. data and concluded that the pulses arose from a fluctuation in one component of an extended red noise in their power spectrum. They then acquired a new longer *EXOSAT* observation but were still unable to detect again a 6 ks signal. Horaguchi et al. (1994) were likewise unable to find this period or any other period up to 13 ks from additional *Ginga* observations. These authors also searched for correlations between variations in the X-ray and UV and optical bands. Their data were based on broadly contemporaneous, not simultaneous, time series and were not able to find correlations.

Haberl (1995) reported the possible existence of a 8.1 ks period in a soft X-ray light curves from 4 clusters of observations distributed over 65 ks. They then examined archival *EXOSAT* data and could not confirm this signal. Due to the limitations of these data, however, they did not believe this was a decisive test. The many X-ray light curves of  $\gamma$  Cas determined in the meantime have not been able to find this period. In addition, this report may be criticized because of the poor time sampling for this short period.

Torrejón & Orr (2001) noticed a sinusoidal variation in an 18.7 ks-long *BeppoSax* light curve of HD 110432. On this basis they claimed the existence of a  $\sim 14$  ks “pulse period.” However, SB06 demonstrated that irregular undulations with a similar timescale also occur in the X-ray light curve of  $\gamma$  Cas, and yet it shows no periodicities. Subsequent light curves of HD110432 have not shown this periodicity but have shown other such undulations, e.g., Lopes de Oliveira et al. (2007b).

In addition to these claims Lopes de Oliveira et al. (2006, “L06”) discovered a 3.2 ks modulation in a light curve of the analog HD 161103, acquired in 2004 with the *XMM*, by identifying 4 (out of a possible 5) maxima. However, such a modulation was not present in subsequent observations carried out in 2012 with the same instrument (Martinez Riberio et al., 2014).

Just as interesting perhaps is the discovery of periodic “near-cessations” in either basal or flare X-ray flux of  $\gamma$  Cas, each lasting just a few minutes. RS00 first report the existence of 7–7.5 hour cessations. An example of a near-cessation is denoted by an upward arrow in Figure 6. These authors did not claim that the cessations are strictly periodic. In fact subsequent light curves have shown such events to occur during some epochs every 7 hours, but occasionally at other time every 3.5 hours and 5.8 hours (Robinson, Smith & Henry, 2002, “RSH02”). Interestingly, from archival *International Ultraviolet Explorer (IUE)* data Cranmer, Smith & Robinson (2000, “CSR00”) have found a “flutter” in the fluxes of the so called Discrete Absorption Components situated in the far blue wings of the CIV and SiIV resonance lines. These recurred with a 7.5 hours. regularity during an *IUE* campaign in January 1982.

Separately, the occurrence of flux cessations hints at the existence of an input energy reservoir which empties over a relaxation cycle (SLM12).

### 3.7. The 70-day cyclical and annualized signals.

Early in the history of monitoring  $\gamma$  Cas in optical and X-ray wavebands, it became clear that the light curves vary on timescales of more than a day but shorter than a year. RSH02 first noticed that optical variations occur that are almost periodic, with an average cycle length of  $\sim 70$  days and a full amplitude of 0.02–0.03 magnitudes in the *V* band. HS12 demonstrated that the cycle properties vary across various degrees of parameter space. Thus, the full range of the cycle lengths is about 50–91 days. The cycles can change their lengths and amplitudes from one cycle to the next. They can even decay

and grow anew in less than a few weeks. In addition, the ratio of amplitudes  $\Delta B/\Delta V$  is variable over the years and may have a bimodal distribution.

RSH02 also found, if suitably scaled X-ray variations of  $\gamma$  Cas from six epochs, that the optical cycles exhibited a very good relation with epochal averages of X-ray flux. This is evident according to Figure 10), at least during this time interval. Using the scaling factor required to match the X-ray and optical variations, SHV were able to anticipate the scale and increase of the X-ray flux over the course of 10 days a few years later. Analyzing 15 years of simultaneous *ASM/RXTE* X-ray data and *V* band APT observations, MLS15 found that on many occasions the regularly sampled X-ray and optical light curves were very well correlated on time scales of several months (see their Fig. 4) while only imperfect correlation was seen during other observing seasons. They noted that the correlation could be improved by broadening the range of timescales from tens of days to several months and applying the same X-ray/optical (disk only) scale factor RSH02 had found to variations over the broader timescale of 70 days to a few years. The correlation for these wavelength regimes for annualized variation-averages is shown for 9 years in Figure 11, left panel. The optical averages come from the ground-based APT system while the X-ray averages come from the *All Sky Monitor (ASM)* experiment carried out by the *RXTE*. Figure 11, right panel, shows the corresponding running averages for the two systems, this time for 15 years, showing that well correlated variations occur on timescales of a year and longer.

The red tinge of the 70-day cycle signal indicates that unlike the gray 1.21 day signal the long cycles originate from a structure cooler than the Be star in the  $\gamma$  Cas system. This can only be its circumstellar disk. These facts argue that the disk is somehow *associated with* the generation of most or all of the hard X-ray flux.

SB06 have shown, albeit from optical photometry over a single season, that a similar red-tinged cycle may exist for HD 110432. It is a longer timescale variability,  $\sim 130$  days, than the cycles associated with  $\gamma$  Cas.<sup>6</sup>

---

<sup>6</sup> It can be noted that  $\sim 70$  day cycles have also been found in the B0.3IV star  $\delta$  Sco. While the phenomenology of these optical cycles has some similarities to those discussed here, there are important dissimilarities as well (Jones et al., 2013). First, the amplitudes are frequently about five times as large as those present in the  $\gamma$  Cas record. Second, the color-brightness phasing can vary widely from cycle to cycle, i.e., from a neutral to correlated to anti-correlated relation. The latter is a distinctly different behavior than the

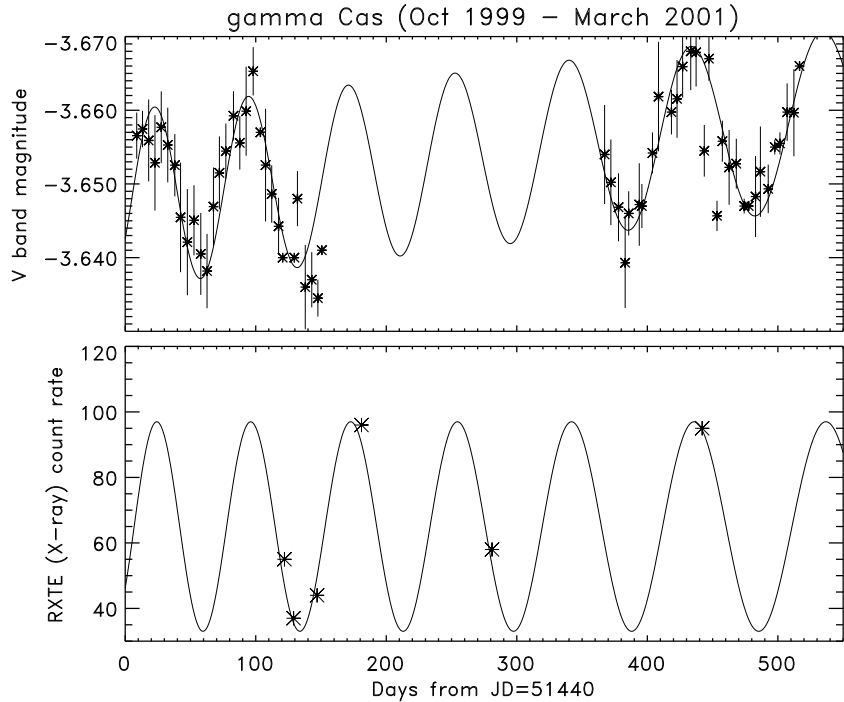


Figure 10: *Top*: A comparison of APT  $V$  band observations of  $\gamma$  Cas with time during 1999–2001 fit to a modified sine curve (solid line). *Bottom*: Trend-removed sine curve fit from top panel to six epochal *RXTE* X-ray observations. After [Robinson, Smith & Henry \(2002\)](#).

### 3.8. Epochal (long-term) changes in the light curves of $\gamma$ Cas and HD 157832.

The first attempt to search the  $\gamma$  Cas X-ray light curve for variations on a timescale of years or longer was made by [Horaguchi et al. \(1994\)](#). These authors found that even when allowance was made for cross-calibration uncertainties among early-generation X-ray satellites, “no particular tendency toward a long-term variation” were seen. Even so, using annual averages of X-ray data, SLM16 have found several year-long minor trends in X-ray fluxes

---

consistently phased relations in the  $\gamma$  Cas light curve. Third, Jones et al. suggest that these variations are caused by the Be star periodically injecting mass to the disk, thereby inducing structural changes. However, no evidence exists that  $\gamma$  Cas injects mass into its disk on any quasi-periodic timescale.

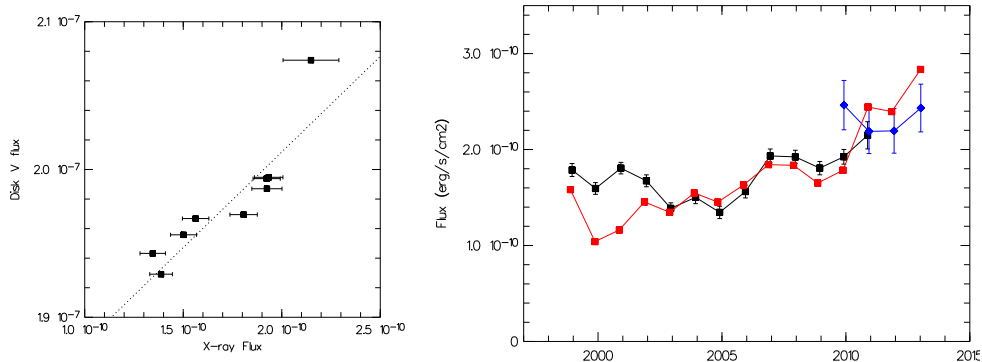


Figure 11: *Left panel:* variations of  $\gamma$  Cas of optical/APT flux estimated for the Be disk alone against X-ray fluxes from the *RXTE* All Sky Monitor program over 9 years. *Right panel:* running annualized flux averages over 15 years for the  $\gamma$  Cas disk (optical, scaled to the X-ray flux range from the relation determined in the left panel) and X-ray data with error bars (from *RXTE/ASM* and, for 2010-2013, from the *Monitor of X-ray Images* instrument on board the International Space Station). APT data are open symbols (in red for on-line version). After [Motch, Lopes de Oliveira & Smith \(2015\)](#).

of  $\gamma$  Cas (see Figure 11b) and optical fluxes that reflect changes in the disk emission. These variations are mild, amounting no more than tens of percent over a few years.

As remarked in the discussion of Figure 3, variations of the *soft* X-ray band flux over long timescales are another matter. First, a factor of three variation was found for  $\gamma$  Cas itself (S04, SLM12) and then over 14 years for the  $\gamma$  Cas analog HD 157832 ([Lopes de Oliveira & Motch, 2011](#)). The  $\gamma$  Cas case is particularly edifying, once again, because the changes in the soft X-ray spectrum can be modeled by variations of more than  $300\times$  in the local  $N_{\text{H}_b}$  absorption column for  $\frac{1}{4}$  of the X-ray site(s). According to SLM12, significant changes were also found in the soft fluxes during the 40-day interval in mid-2010 over which  $\gamma$  Cas initiated a larger than average optical “Be outburst” in terms of increases in the  $\text{H}\alpha$  emission strength and dimming and reddening of photometric magnitudes. In fact, as shown in Figure 12, the four closely spaced *XMM* spectra observed in 2010 reinforce a correlation between reddening and column density through the soft X-ray attenuation also seen for the 2001 and 2004 observations. This led SLM12 to conclude that foreground gas escaping the Be star during outburst events absorbs preferentially soft X-rays along our line of sight to the star through photoelectric absorption.



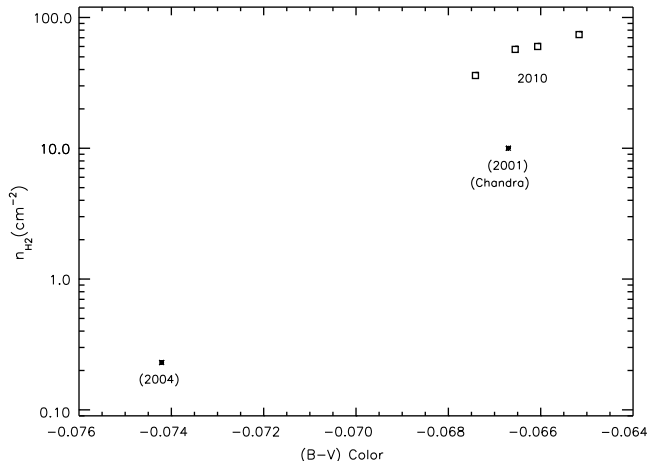


Figure 12: The observed optical  $(B - V)$  color magnitude against modeled  $N_{\text{H}}$  column density (in units of  $10^{22} \text{ cm}^{-2}$ ) for  $\gamma$  Cas, modeled for *XMM* and *Chandra* spectra. The increased  $(B - V)$  reddening is caused by a continuing build up of the inner Be decretion disk as a result of injections of matter into the circumstellar environment. After [Smith et al. \(2012\)](#).

#### 4. The $\gamma$ Cas analogs.

The study of the X-ray emission of  $\gamma$  Cas has taken a new direction with the realization in the last decade when new early-type Be stars were discovered with similar X-ray properties (M07, SB06; L06; L07b). At last, its emission could be compared to those of other stars in relevant parameter spaces. These additions revealed characteristics that turn out to be narrowly distributed not only in the X-ray domain but also with respect to spectral type, rotation rate, and evolutionary state. In addition the presence of  $\text{H}\alpha$  emission in the spectra of all these stars indicates the presence of well developed decretion disks.

Assembling information from the literature, [Smith, Lopes de Oliveira & Motch \(2015\)](#) constructed a catalog of members of the  $\gamma$  Cas class, given here as Table 2. The table lists star name, spectral type, status of  $\text{H}\alpha$  Violet and/or Red emission lobe (*s* for single-lobed, *d* for double-lobed – this is a proxy for the inclination of the star-disk plane), equatorial  $v \sin i$  from line broadening, equivalent width of the  $\text{H}\alpha$  line, binarity (SB1) or blue straggler status (if known),  $V$  magnitude, the energy temperature of the primary plasma ( $kT_{\text{hot}}$ ), the X-ray luminosity (taken usually in the range 0.2–10 keV,

which we refer to as  $L_{x_{0.2-10}}$ ), and the citation to the first paper in which the X-ray fluxes were highlighted as reminiscent of  $\gamma$  Cas behavior. We discuss each of these stars in order of their appearance in this table. We have also added 3XMM J190144.5+045914 from the recent *XMM-2MASS-GLIMPSE* cross correlation catalog (Nebot Gómez-Morán et al., 2015, “N15”).

Table 2: Designated and candidate  $\gamma$  Cas stars and some important properties. (After Smith et al. 2015.)

Star Name	Sp. Type	(Lobe) $v \sin i$ $\text{km s}^{-1}$	$\text{EW}_{H\alpha}$ ( $\text{\AA}$ )	SB1? (Blue Str.)	$V$ mag	$kT_{\text{hot}}$ (keV)	$L_X \times 10^{-32}$ ( $\text{erg s}^{-1}$ )	Ref.
$\gamma$ Cas	B0.5 IV-Ve	(d) 385	-34	SB1	2.39	12–15.7	7–11	(1)
HD 110432	B0.5 IIIe	(d) 350	-52	BS	5.31	16-37	4.2–5.2	(2)
HD 161103	B0.5 III-Ve	(s) 224	-31	–	8.69	7.4–10	4–6:	(3)
SAO 49725	B0.5 III-Ve	(s) 234	-30	–	9.27	12.3	4–12:	(3)
HD 119682	B0.5	220	-30	BS	7.91	10.4	6.2	(4)
SS 397	B1 Ve	–	-34	–	11.76	6.3–13	3.4	(5)
NGC 6649 WL9	B1-1.5 IIIe	–	-36	BS	11.9	10	5	(5)
*XGPS-36	B1 Ve	–	-27	–	14.3:	10	3.4	(6)
HD 157832	B1.5 Ve	(d) 217-266	-25	–	6.6	10–11.3	1.3-3.4	(7)
HD 45314	B0 IVe	285	-30	SB1?	6.6	21	$L_X/L=-6.1$	(8)
*TYC3681-695-1	B1-2 III/Ve	–	-31	–	11.36	–	1.4-5.8	(9)
*2XMMJ ... 180816.6-191939	B0 Ve	–	-50	SB?, BS?	22:	–	2.4–3.3	(9)
*3XMMJ ... 190144.5+045914	O9e-B3e	–	–	–	–	–	0.4–3.0	(10)

Notes: (1) White et al. (1982), (2) Smith & Balona (2006), (3) Lopes de Oliveira et al. (2006), (4) Rakowski et al. (2006), (5) Motch et al. (2007), (6) Motch et al. (2010), (7) Lopes de Oliveira & Motch (2011) (8) Rauw et al. (2013), (9) Nebot Gómez-Morán et al. (2013), (10) Nebot Gómez-Morán et al. (2015).

\*These are “candidate” objects (see text).

#### 4.1. X-ray spectra and optical properties.

##### 4.1.1. HD 110432: the first “analog.”

As the first discovered and brightest analog excluding  $\gamma$  Cas itself, this star is the next most studied in the X-ray regime. This X-ray source was first found in a HEAO-1 All Sky Survey, and its optical counterpart was identified as HD 110432 by Codina et al. (1984). The star is probably a member of the Galactic cluster NGC 4609. If so, considering its position on the HR Diagram, it is likely to be a blue straggler (Marco, Negueruela & Motch, 2007). From the presence of the Fe XXV/XXVI blend in a *BeppoSax*

spectrum and the afore-mentioned claim of a 14 ks “pulse” period, [Torrejón & Orr \(2001\)](#) put forward this B0.5 III star as a binary Be + WD candidate. However, the star was first proposed (SB06) to be a “ $\gamma$  Cas analog” on the basis of its hard X-ray spectrum, the undulations of its X-ray light curve, and the similarity of its optical spectrum to  $\gamma$  Cas. As noted next, the X-ray emission properties, while qualitatively similar to  $\gamma$  Cas, exhibit somewhat different  $kT_{\text{hot}}$  values and thus gave the first rough estimate of the range of properties in this class.

Two reliable moderate and high resolution X-ray analyses have been carried out, first by L07b on the basis of three serendipitous *XMM/EPIC* observations (limited to wavelengths  $\leq 21 \text{ \AA}$ ), and second by [Torrejón, Schulz & Nowak \(2012, “TSN12”\)](#), who observed this star with *Chandra/HTEG*. The HTEG yields good signal to noise ratios over the wavelengths 1.6–16  $\text{\AA}$ . These studies were able to establish clearly thermality in the plasma by demonstrating the existence of three plasma components. However, the values of the respective plasma temperatures were different in the two studies ( $kT_{\text{hot}} = 16\text{--}37 \text{ keV}$  versus  $16\text{--}21 \text{ keV}$ ,  $kT_{\text{warm}} = 3\text{--}6 \text{ keV}$  versus  $7\text{--}8 \text{ keV}$ ,  $kT_{\text{cool}} = 0.2\text{--}0.7 \text{ keV}$  versus  $0.2 \text{ keV}$ ). Clearly the value of  $kT_{\text{hot}}$  varies substantially over with time for this object, and probably the temperatures of the warm and cool plasmas as well. For both studies the hot plasma emission measure comprised about 80% of the total, which is a similar fraction as we found already for  $\gamma$  Cas. TSN12 also obtained and analyzed *Suzaku* spectra, which extended the energy coverage to 70 keV. These data disclosed the presence of an energy tail that could not be modeled by a 14 keV  $kT_{\text{hot}}$  plasma component alone. Moreover, fitting both spectra over the entire energy range, these authors found that in addition to the ISM contribution two columns were needed to preserve the thermal assumption, one applicable to the very hot component and the other to the warm component. These data discovered a hard energy tail out to 33 keV in addition to the hot thermal component. The nature of this tail, whether thermal or nonthermal, is so far unresolved. TSN12 were also in agreement with L07b that the spectrum of this object is likely to be variable over time.

Flare lifetimes as short as 10–15 s are observed in the light curve of HD 110432 (L07b), again, suggesting a density of  $\sim 10^{14} \text{ cm}^{-3}$  at the sites of their formation. The *rif* components of Si XIII and SXV suggest either high densities (if radiative quenching from UV radiation of a nearby star is unimportant) or, to insure these radiative effects are minimized, a distance of less than  $2R_*$  above the Be star for the hot plasma.

Another interesting property determined in the spectrum is the pattern of elemental abundances. Similar to the case of  $\gamma$  Cas, the [Fe] determined from Fe L shell ion lines is only slightly subsolar whereas the [Fe] found from the K-shell lines is definitely low, e.g.,  $0.3Z_{\odot}$ , though not quite so low as the  $\gamma$  Cas values in our Table 1 (L07b). In addition, TSN12 found that their models underpredicted emission strengths of Na XI, Ne X and Fe XVII lines, but it is not yet clear that these signify anomalous abundances.

A final interesting property of the emission line spectrum is the large turbulent velocity of  $1200 \text{ km s}^{-1}$  TSN12 measured the recombinational Fe K lines. This is even larger than the velocities S04, L10, and S12 ( $200\text{--}950 \text{ km s}^{-1}$ ) found for lines arising from less excited ions in X-ray spectra of  $\gamma$  Cas. The velocity found for HD 110432's Fe K-shell lines is interesting because it is near the velocities posited in SRC98's flare model of exploding parcels.

#### 4.1.2. HD 119682.

HD 119682 is a Be star which was first identified as the optical counterpart of a *ROSAT* source (Rakowski et al., 2006; Safi-Harb et al., 2007, L07b). Although the star's position in the HR Diagram makes it appear as a young star, its kinematic properties and its position in the sky suggests that it is a blue straggler member of the Galactic cluster NGC 5281, and therefore has an age of  $40 \pm 10$  Myr (e.g., SH07; ?). The spectral type of this star is not yet well agreed upon. Line-blanketed synthesis models of its optical spectrum suggest a type of O9.7 (Martins, Schaerer & Hillier, 2002), while SH07 adopt B0.5. Initial studies of *Chandra*/HTEG and *XMM*/EPIC by Rakowski et al. (2006), Safi-Harb et al. (2007), and Torrejón, Schulz & Nowak (2013) agree that the X-ray continuum is best fit by two plasma components, one hot (14.5-15 keV) and the other cool ( $\approx 0.2$  keV). They also found an absorption column consistent with the ISM value. These studies reported difficulty in finding spectral emission lines. However, on the basis of additional *Chandra* data, G15 demonstrated that the apparent absence of the Fe complex in earlier studies was at least partially due to inadequate photon statistics in the extant spectra. We suspect also that the Fe abundance derived from lines from the K-shell ions is subsolar. Torrejón, Schulz & Nowak (2012) found that a single absorption column was necessary to fit their data. They argued that this is consistent with their finding that the Be star-disk system is viewed almost pole-on.

#### 4.1.3. HD 161103.

HD 161103 (B0.5III-Ve) was found to have an anomalous X-ray luminosity from the *ROSAT* All Sky Survey data (Motch et al., 1997). L06 acquired *XMM/EPIC* spectra to investigate it further. The X-ray data suggest  $L_{X_{2-10}} \sim 1 \times 10^{32} \text{ ergs s}^{-1}$ , a hard spectral slope, and that the Fe line complex is present. Using the same data, L06 and G15 found that two thermal plasma components are necessary for a good fit to the data. L06 found  $kT_{\text{hot}} = 8.0 \pm 1.0 \text{ keV}$  and  $kT_{\text{cool}} = 0.76 \pm 0.2 \text{ keV}$ . Only a single absorption column was necessary, according to models fitting the X-ray spectra. It is consistent with the ISM column inferred from  $E(B - V)$  reddening. As with  $\gamma$  Cas the Fe abundance determined from the K-ion lines is probably quite low.

#### 4.1.4. SAO 49725.

Like HD 161103, SAO 49725 is a B0.5III-Ve star that was identified as an early type star with a high X-ray luminosity in the *ROSAT* All Sky Survey data (Motch et al., 1997). L06 acquired *XMM/EPIC* spectra to investigate it further. The X-ray data suggest  $L_{X_{2-10}} \sim 1 \times 10^{32} \text{ ergs s}^{-1}$ , a hard spectral slope, and that the Fe line complex are present. As for HD 161103 both L06 and G15 both found that two thermal components were necessary. L06 found that  $kT_{\text{hot}} = 12.8_{-3.4}^{+7.7} \text{ keV}$  and  $kT_{\text{cool}} = 0.87_{-0.25}^{+0.5} \text{ keV}$ .

G15 found that two thermal components were necessary for a good fit to the data, namely 18.86 keV and 0.82 keV. The column density from the X-ray spectrum is consistent with the ISM column inferred from  $E(B - V)$  reddening. Again, as with  $\gamma$  Cas the Fe abundance determined from the K-ion lines is probably quite low.

#### 4.1.5. SS 397; 2MASS J18332777-1035243.

This B0.5Ve star is also known as 2XMM J183327.7-103523 and the IR source 2MASS J18332777-1035243. M07, L06, and L07a have identified it as a  $\gamma$  Cas analog. These authors found its  $kT_{\text{hot}}$  to be consistent with 9–14 keV. The star's  $L_{X_{0.2-12}}$  is  $\sim 4.4 \times 10^{32} \text{ ergs s}^{-1}$  (N13). The *XMM* spectrum of SS 397 also exhibits evidence of thermal Fe lines. The  $H\alpha$  line in the spectrum has an equivalent width of  $-31 \text{ \AA}$ .

#### 4.1.6. NGC 6649, WL9; 2MASS J18332830-1024087.

This B1-1.5 IIIe star is the brightest star in the cluster NGC 6649, according to Motch et al. (2003). These authors and Marco, Negueruela & Motch (2007) judged the star to be a likely blue straggler. The X-ray source was first

designated as 2XMMJ183328.3-102407 and the optical component as either USNO0750-13549725C or 2MASS J18332830-1024087. L06 declared it to be a  $\gamma$  Cas analog based on *XMM/EPIC* spectra. The N13 catalog reported an X-ray luminosity,  $5 \times 10^{32}$  ergs $^{-1}$ , also consistent with the X-ray emission of a  $\gamma$  Cas analog. L07a found that the spectrum was thermal, based on the presence of blended Fe XXV/Fe XXVI lines. L07a found that the data quality permitted a determination of only a single plasma component, consistent with  $kT \sim 11$  keV.

#### 4.1.7. \*XGPS-36; GSC2 S300302371.

Also known as 2XMM J011559.0+90914 and (optical counterpart) GSC2 S300302371, according to [Motch et al. \(2010\)](#), this star has a spectral type near B1Ve and an H $\alpha$  emission EW  $\sim 27$  Å. Assuming a distance of 2–4 kpc, these authors estimated an X-ray luminosity  $L_{X_{0.2-12}} \approx 3.4 \times 10^{32}$  ergs s $^{-1}$ . They also found that *XMM/EPIC* spectra can be fit with  $kT \sim 10$  keV.

#### 4.1.8. HD 157832.

Of the known  $\gamma$  Cas stars HD 157832 is the latest spectral type, B1.5 Ve (possibly B2) according to a detailed analysis of its optical spectrum by [Lopes de Oliveira & Motch \(2011\)](#). Modeling of *XMM/EPIC* data suggests a thermal, two-component model, with  $kT_{\text{hot}} \approx 11.25$  keV and  $kT_{\text{warm}} \approx 2.3$  keV. The *XMM/EPIC* spectra exhibited the presence of the full Fe complex. These authors suggested that long-term changes in the X-ray flux is consistent with changes in a local absorption column,  $N_{\text{H}_b}$ .

#### 4.1.9. HD 45314.

HD 45314 is another X-ray source with an especially hot plasma energy temperature of  $21 \pm 6$  KeV, according to ([Rauw et al., 2013](#)). The full Fe complex presented in the G15 compendium of *XMM/EPIC* data for this star clearly shows the star’s  $\gamma$  Cas-like nature. The short (24 ks) *XMM/EPIC* observation made by these authors does not offer good signal-to-noise in order to derive information about the presence of a secondary X-ray emitting plasma. Rauw et al. found just marginally different flux levels compared to an earlier *EXOSAT* observation and thus were unable to judge whether the star’s flux had actually changed.

Although we cite these authors’ spectral type of B0e IV star HD 45314, we also note that [Sota et al. \(2011\)](#) assign a spectral type as early as O9:npe.

4.1.10. \*TYC3681-695-1; 2MASS J01155905+590411.

This star is also known as 2XMMJ011559.0+590914 and (optical counterpart) 2MASS01155905+5909141. N13 classified it as a B1-2 III-Ve star. This is uncertain because of its large ISM reddening. However, the strong H $\alpha$  equivalent width (EW  $\sim$  -31 Å) suggest it is a Be star. These authors also found that  $L_{X_{0.2-12}} = 1.4-5.8 \times 10^{32}$  ergs s $^{-1}$ , which is characteristic of  $\gamma$  Cas analogs. Furthermore, the X-ray spectrum is hard (Motch, 2015).

4.1.11. \*2XMM J180816.6-191939.

First considered a possible HMXB system by Motch et al. (2003), Motch et al. (2010) obtained additional optical spectra in an attempt to determine its spectral type, but they could not identify absorption lines to determine a spectral type. They determined a rough luminosity based on estimated reddening. This luminosity is consistent with a main sequence spectral type of B0. They also found that  $L_{X_{0.2-12}} \sim 3.3 \times 10^{32}$  ergs s $^{-1}$ , given an assumed distance of 6–7 kpc. This fact led the authors to advance this star as a  $\gamma$  Cas-candidate analog. Assuming its estimated spectral type is confirmed by optical spectra, its Fe XXV/Fe XXVI line emissions are also not yet well constrained.

4.1.12. \*3XMM J190144.5+045914; 2MASS J19014455+0459147.

N15 cross-correlated the 3XMM, GLIMPSE, and 2MASS surveys and isolated the source 3XMM J190144.5+045914, aka 2MASS J19014455+0459147, as a hard X-ray source with a  $L_{X_{0.2-12}} = 0.4-3.0 \times 10^{32}$  ergs s $^{-1}$  and a column density of  $N_{\text{H}} = 2.7 \pm 0.2 \times 10^{22}$  cm $^{-2}$ . Its spectral type measured by IR Brackett lines is in the vicinity of O9e-B3e, according to the infrared line-spectral type calibration of Steele & Clark (2001). N15 categorically classified this source as a  $\gamma$  Cas analog. The spectral type of the star is not accurately defined, nor is the extant X-ray spectrum is not well enough exposed to distinguish between a power law or a thermal continuum, nor does it show evidence of FeK lines. However, the XMMFITCAT database (Corral, Georgantopoulos & Watson, 2014) reports satisfactory thermal fits with  $kT \approx 9.1 \pm 3$  keV and  $N_{\text{H}} = 3 \pm 0.5 \times 10^{22}$  cm $^{-2}$ . The values of energy temperature, X-ray luminosity, and spectral type are consistent with  $\gamma$  Cas analogs.

## 5. Summary of properties.

From the characteristics of members of the  $\gamma$  Cas class we may summarize the properties as they now appear.  $\gamma$  Cas stars are first of all classical Be stars with spectral types in the range  $\approx$ O9.7–B1.5 and luminosity class from III to V, and current strong H $\alpha$  emission.

It is now fair to say that *if the X-ray spectrum of a Be star satisfying the above optical criteria and also indicates the presence of thermal plasma, i.e. visible Lyman  $\alpha$  lines of Fe XXV and Fe XXVI, a continuum slope consistent with an energy temperature needed to produce them ( $kT \gtrsim 10$  keV), then it can be advanced as a  $\gamma$  Cas star. The spectrum should also exhibit at least a weak Fe fluorescence feature (assuming a detectability  $EW(\text{FeK}\alpha) \sim 30$  eV), and the star's  $L_X$  should be  $10^{32}$ – $10^{33}$  ergs  $s^{-1}$ . If the detectability of thermal FeK lines is relaxed, as must be the case for four stars in our Table 2, marked with a “\*” symbol, then we will refer to them as “candidates.” If the lines are ultimately detected, the “candidate” qualifier should be dropped and the star be promoted to full member of the  $\gamma$  Cas class.* A remaining task before us is to determine whether the  $L_X$  criterion and spectral hardness are sufficient as well as necessary conditions.

Of the analog stars in our Table 2 only HD 110432, HD 119682, HD 45314, and perhaps HD 157832 are bright enough to have been examined so far at high dispersion and at softer X-ray energies than 1 keV. In these cases it is clear that at least one cooler secondary plasma is required to fit the spectrum. Similarly, the existence of mild variability - especially rapid though variability due to “flares” is probably required. However, one cannot add the requirement that the class should fulfill certain variability criteria, or they would not be discovered from X-ray surveys as they have been recently. In the event of multiple observations over long timescales one should insist that any variability be small, much smaller for example than in most accreting sources. Other properties such as a subsolar Fe abundances from the Fe XXV and Fe XXVI lines may also be common if not universal, but this too must be investigated.

Determining the physical *cause* of the hard X-ray emission is another matter. We will argue in §6 that, alone, even X-ray observations of superb quality and time coverage are insufficient to point to a specific mechanism for the generation of the X-rays.



## 6. Suggested scenarios for X-ray generation.

### 6.1. Accretion onto a degenerate star or its disk.

#### 6.1.1. Consideration of the WD accretion scenario (pro and con).

The seminal paper of [White et al. \(1982\)](#) was pivotal in focusing the X-ray community’s attention to  $\gamma$  Cas, although not necessarily for what one might regard today as prescient reasons. These authors highlighted the similarity of the optical spectrum of this star to that of the prototypical Be X-ray pulsar system X Per. Also, the presence of a bright nebula surrounding the star ([Poeckert & van den Bergh, 1981](#)) suggested to these authors that the then-putative secondary of the  $\gamma$  Cas system is a supernova remnant and therefore is currently a neutron star. Alas, the authors found no pulses in the X-ray light curve. On the other hand, they discovered no FeK feature or evidence of thermality in the spectrum either, which they might have interpreted as being a result of accretion onto a WD. An interesting sidenote is that, from the first, these authors recognized that if the X-ray spectrum is thermal it means the plasma has  $kT \approx 12$  keV, i.e., the currently accepted value. In any event, they noted that the instrumental limitations existing at that time precluded them from detecting intermediate timescale periodicities. Moreover, they did not anticipate the presence of rapidly evolving “flares.”

[White et al. \(1982\)](#) utilized the Bondi-Hoyle accretion radius estimated for a hypothesized secondary in the vicinity of the Be star and were the first to underscore the difficulty of powering a luminosity  $L_X \sim 10^{33}$  ergs $^{-1}$  by Be wind-powered accretion onto a WD. Moreover, they emphasized that such emission was unlike that found for OB stars, which at that time was linked to a so-called “coronal model” of [Marlborough \(1977\)](#). Altogether, they understood these arguments to favor the accretion NS scenario. Then, as noted repeated claims of periodic “pulses” in the light curves of various  $\gamma$  Cas analogs for several years kept alive this scenario (e.g., [Safi-Harb et al., 2007](#)). However, the failure of subsequent investigations to validate claims of pulses has since viscerated this argument. As already noted, M86 unravelled the NS argument further with their finding that the X-ray spectrum of  $\gamma$  Cas is thermal. By contrast Be-NS systems exhibit no or at most weak FeK Lyman  $\alpha$  features, whose presence are indicative of thermality, in their spectra (M07, M86, G15).

M86 considered key characteristics of flares to argue for their formation on the surface (or accretion column) of a WD. These attributes included the emission measures of the flares as well as their high plasma temperatures,

optical thinnesses, and short durations. In the latter case they assumed their short lifetimes arise from cooling in a high density medium. The permitted region in the flare-emitting blob’s radius is consistent with a WD’s radius, and this was used in support of the WD accretion hypothesis.

The problem with the latter argument is that it is a necessary but not sufficient condition. Many individual flares may occur over an extended surface area, but this does not mean they are generated one at a time over the same contiguous surface, e.g., of a WD. To the contrary, one can argue that the occasional confluence of flares, including individual flares having different colors, indicates it is likely that they are distributed over a projected area larger than a WD.

K98 amplified the WD argument from analysis of moderate dispersion *ASCA* spectra of  $\gamma$  Cas. Their results confirmed that the X-ray light curve typically contains ubiquitous short-lived flares while its spectrum is hard and contains the FeXXV and FeXXVI emission lines. Moreover, these authors took the absence of X-ray pulses to indicate that any existing WD cannot be strongly magnetic.

K98 noted dissimilarities of the X-ray spectrum of  $\gamma$  Cas with X-ray coronae in late-type active or T Tauri stars, which exhibit a continuum and emission line pattern consistent only with cooler plasma. They also contended against the contemporary SRC98 picture as they understood it and argued further against any “coronal” model. However, SRC98 had not argued for a coronal model because they emphasized the X-ray flux is generated in a much denser medium.

In addition, K98 argued that SRC98 did not consider that the light curves of dwarf nova binaries such as SS Cyg could in principle also exhibit an UV/X-ray anticorrelation such as that found in Figure 6. However, SS Cyg is actually a close low-mass binary ( $P_{\text{orb}} = 6.6$  hours), consisting of a Roche lobe-overflowing K5 V star and a WD that hosts an accretion disk. The system undergoes irregular UV/EUV outbursts lasting on the order of a week. Typically, just before an EUV outburst the X-ray flux decreases and its hardness changes as well. An analogous mid-UV outburst occurs shortly thereafter. Thus, importantly, the changes in these bands do not occur simultaneously. In fact, the asynchrony of changes across the energy range is explained well by the accretion disk dissipation model for dwarf novae. According to this model when an outburst begins, an instability results from the accumulation of matter at the outer edge of the accretion disk and migrates to its inner edge. This causes sequential brightening in one waveband after an-

other. None of these properties is shared by the synchronous anti-correlation exhibited in Figure 6 and Figure 9.

K98 also argued that because flares can be excited on some active WDs, their existence on  $\gamma$  Cas does not exclude a Be-WD accretion scenario. The best example of WDs with flares in their light curves, so-called “intermediate polars.” Intermediate polars are binary systems consisting of an evolutionarily-driven, expanding main sequence star and a magnetic WD. Mass from the primary is transferred by angular momentum conservation to an accreting disk around the WD. Matter is then guided by magnetic fields to an accretion column at the disk-star interface. Initially falling into this column as blobs, these structures are stretched vertically by tidal forces. They shock and emit high energy radiation when they eventually brake at high densities, emitting flares. Flares are observed primarily only at certain orbital phases. Studies by [Beardmore & Osborne \(1997\)](#) and [Schwarz et al. \(2005\)](#) have found that X-ray colors of flares can be quite different among various polars. They attribute this difference to the characteristic blob size of a particular polar. In the case of AM Her small blobs shock near the top of the accretion column, where they can be observed by an external observer as moderately hard ( $\sim 3$  keV) individual flares. In other cases, such as V1309 Ori, the blobs are larger and their infalls survive the fall through most of the column to the WD’s surface. The overlying column absorbs the emitted X-ray flux, and all that is observed, if visible at all, are aggregates of unresolved soft X-ray events. (For a review see [Mouchet et al., 2012](#)). However, notice the near equality of the colors of most basal and flare fluxes in  $\gamma$  Cas and HD 110432 is in direct contrast to the diversity of flare colors observed among polars. In addition, the observation of ubiquitous flaring in the  $\gamma$  Cas stars’ light curves is in disagreement with the observed phase-dependent events in polar light curves. In summary, the flare characteristics of  $\gamma$  Cas are not a good fit to the characteristics of polars.

### *6.1.2. Orbital-rotational relations.*

[Corbet & Mason \(1984\)](#) discovered that Be-NS binaries follow a strong correlation between rotational and orbital periods, where the latter were determined from their X-ray pulse rates. They also showed that this correlation can be predicted by orbiting particles around a strongly magnetized neutron star being balanced between centrifugal and magnetic forces at points where the corotation and Alfvén radii are equal. The determination of periods for additional Be-NS systems over the years has confirmed Mason & Corbet’s

results, and thus the so-called Corbet relation has been a useful tool in predicting one period or the other when only one is known. Building on this result, [Apparao \(1994\)](#) has applied the Corbet relation for Be X-ray binaries with shorter pulse periods. His reasoning was that shorter pulse periods might be expected for Be-WD systems because of the larger radii and weaker field strengths of white dwarfs. Apparao found that two binaries in his sample fell on a line in the  $P_{orbit}-P_{rot}$  plane well to the left (towards shorter orbital periods) where most Be-NS systems reside. He argued that the shorter orbital periods occur because the degenerate secondary stars have weaker fields than NS do, and he took these as possible Be-WD binaries. [Apparao \(2002\)](#) found next that the 204 day orbital and  $\sim 1$  day *rotational* periods of  $\gamma$  Cas fall close to the putative Be-WD relation and therefore that systems falling along it can be considered candidate Be-magnetic WD systems. In assessing this hypothesis, one can point out that no evidence has since been uncovered to confirm that Apparao’s sample of two are in fact Be-WD systems. Indeed, in the intervening years no Be-WD systems have been found that emit hard X-rays. Also, in a review of the status of the Corbet relation [Knigge, Coe & Podsiadlowski \(2011\)](#) find a similar subpopulation to Apparao’s. However, they judge it to be secondary population of Be-NS, not Be-WD, systems. It is worth emphasizing again that recent evidence demonstrates that robust “pulses” are not present in the X-ray light curves of  $\gamma$  Cas or its analogs.

### 6.1.3. Super-soft X-ray sources associated with Be stars?

According to the theoretical models of [Raguzova \(2001\)](#),  $\sim 70\%$  of all Be stars could be formed during late stages of binary evolution as a result of angular momentum-rich material migrating through the Roche lobe, accreting to and spinning up the surface layers of the Be star. If so the typical secondaries are white dwarfs with  $T_{eff} \sim 40$  kK. The fact that such secondaries are so much fainter than B stars, even in the UV, is one reason for the general failure to find such systems. If so, one asks: what would they look like in the X-ray domain? Might Be-WD systems be, for example, a subclass of so-called Super-Soft X-ray Sources (SSS)? Could these be related to or confused with  $\gamma$  Cas stars?

SSS are thought to represent a broad class of very soft X-ray emitters that are detected at energies only below 1 keV ([Kahabka & van den Heuvel, 1997](#)). They occur mainly in binaries, including subclasses of novae and polars, but they can be found also among evolved single stars (nuclei of Planetary Nebulae and cooling NS). Under the right conditions nuclear burning occurs when

matter from an evolving primary falls and accumulates onto the WD surface. Upon thermalization of the released potential energy a “super-soft” ( $kT < 100$  eV) black body spectrum-like is emitted. The X-ray flux is strongly attenuated by a dense accretion disk around the WD. Although this makes it difficult to determine the intrinsic  $L_X$  of the source accurately, typical estimates lie in the range of  $10^{36}$ – $10^{38}$  ergs  $s^{-1}$ . Recently survey work has uncovered one SSS associated with an early-type star in each of the Magellanic Clouds, detailed as follows.

[Kahabka et al. \(2006\)](#) discovered the source XMMU J052016.0-692505 in the *XMM/EPIC* public archive and identified its optical counterpart as the Large Magellanic Cloud star LMCV2135. Optical spectroscopy revealed that this to be an early Be giant star that hosts an extensive disk. Moreover, UV filter magnitudes from the *XMM* Optical Monitor are consistent with a photometric spectral type of a B0-B3 III star and a mass near  $16 M_{\odot}$ . At the time of this discovery a Be star with a super-soft X-ray spectrum was a novelty. Thus, they concluded that this SSS Be system is unique and that its X-rays resulted from thermal runaway of matter steadily accreted onto the surface of a WD. If so, it has become the first known Be-WD system. The authors bolstered their argument by showing that the evolutionary-determined ages and the masses estimated for the binary components are consistent with evolutionary scenarios predicted by [Raguzova \(2001\)](#) models for high mass binaries. In sum, these authors argued that SSS objects are a logical channel for Be stars that have been spun up by binary mass transfer. Indeed the spinning up of Be stars in close binaries appears to be a common occurrence, according to a study of Be stars observed in open clusters ([McSwain & Gies, 2005](#)).

Recently [Sturm et al. \(2012\)](#) conducted a survey for SSS in the Small Magellanic Cloud and discovered the SSS object XMMU J010147.5-715550 and determined its optical counterpart to be AzV 281, an O7 IIIe–B0 Ie star. Using arguments similar to those of [Kahabka et al. \(2006\)](#), they concluded that this is another Be-WD system. In addition, X-ray monitoring of the object disclosed the unique circumstance that its soft band (0.2-1.0 keV) flux decreased by a factor of  $\gtrsim 40\times$  in roughly a year.

Neither of these authors suggested a connection between  $\gamma$  Cas and SSS objects. Indeed [Kahabka et al. \(2006\)](#) drew a contrast between the two on the basis of the very softness of SSS star spectra. In addition, the principal sculpting agent of X-ray spectra of SSS Be star binaries is the dense accretion disk surrounding the secondary star; there is no apparent role for the

decretion disk of the Be star. Altogether, there is scant if any evidence for a connection between the two groups of objects.

To conclude this section, the NS accretion hypothesis has lost its early luster in favor of the still-surviving WD one. The surviving appeal of the WD picture lies in the similarity of its spectrum to certain types of active white dwarfs (especially intermediate polars) and the absence of pulses in either  $\gamma$  Cas itself or its analogs. A lingering problem with the WD accretion scenario, as noted by [White et al. \(1982\)](#), has been the question of whether the powering of the observed  $L_X \sim 10^{33}$  ergs $s^{-1}$  can be accomplished from matter accreted from a WD in a  $\gamma$  Cas-like orbit. Estimates in the recent X-ray binary literature (e.g., [Sturm et al., 2012](#)) suggest a range of  $10^{29}$ – $10^{33}$  ergs $s^{-1}$ . The upper limit to this range assumes rapid expulsion of matter in the plane of the disk by a discrete ejection - since it must be orders of magnitude above a wind mass loss rate. Part of the issue has been the uncertainty of the outflow velocity that discrete ejections have. This is important because the mass loss and hence putative accretion-powered  $L_X$  increases as  $1/v_{outflow}^3$ , according to the Bondi-Hoyle accretion formalism. Probably a more relevant question is how efficiently the outer edge of the disk of a  $\gamma$  Cas star is truncated by the tidal interactions with a binary companion (see §1.3.3) and whether discrete mass ejections can cross such a barrier rapidly enough before dispersing to the ISM or returning to the Be star. Although this issue is not yet decisively resolved, so far the evidence does not favor rapid crossings, if such crossings occur at all (e.g., [MLS15](#)). In any case, the optical variations resulting from a strong Be outburst are seldom events. They do not occur in a continuously-repeating or sustained manner, e.g., ([Pollmann, 2014](#); [Henry & Smith, 2012](#)), such as would be required to power the full observed X-ray luminosity of  $\gamma$  Cas.

## 6.2. *The Magnetic Star-disk hypothesis.*

### 6.2.1. *Description.*

Much of the advocacy for the picture of accretion onto a degenerate companion has been made by attempting to tie the  $\gamma$  Cas case to other classes of X-ray Be binary systems for which the accretion model has been so successfully applied. In this section we argue that overall this is insufficient because the  $\gamma$  Cas stars comprise a unique class, one which associates X-ray properties to the immediate environment of the Be star rather than to a binary companion. With this as context, we introduce the so-called magnetic star-disk interaction picture. We preface our discussion by pointing out that this

is a hypothesis built on the empirical data alone. It is supported by a few conjectures, as we will see, and it is not yet capable of making predictions.

The original hypothesis drew its support from correlations of properties of X-ray and UV/optical diagnostics. The first multi-wavelength correlated event was an X-ray flare in the *Copernicus* light curve of  $\gamma$  Cas reported to Peters (1982) in 1978. This coincided with short-lived emissions in the UV resonance lines of Mg II and Si IV and also an H $\alpha$  emission “flare” (Slettebak & Snow, 1978). However, this was a single event. The best continuing array of events was the simultaneous UV/X-ray campaign in 1996. The X-ray/UV correlations reproduced in Figures 6–8 suggested a picture of short-lived corotating cloud complexes ejected from active sites on the Be star (see §3.1.5). Next, the discovery that the 50–91 day cycles are present in both the optical and X-ray region (Figure 10), together with their amplitudes being about larger in the red than the blue, suggested that the cycles originate in the cool Be decretion disk (RSH02). As noted, MLS15 showed that this initial finding can be broadened to demonstrate that optical and X-ray variations of even a year or longer are well correlated, with zero delay and with the same scaling factor applying to this broadened range. Importantly, the zero delay is at variance with the several year delay expected in the accretion scenario between the optical outburst, marking ejection of matter from the Be star and the corresponding X-ray surge due to accretion onto the remote companion. Since the optical variations are well understood to arise from the development of the inner regions of the Be decretion disk, a reasonable conclusion is that the reservoir responsible for hard X-ray energy generation is associated with this structure. *From this inference the concept of a magnetic interaction between the Be star and its disk was born, a picture that is sure to evolve further with new discoveries.*

In brief, the scenario is as follows. By hypothesis, magnetic field lines extend from points on the Be star’s surface, at first in the form of small-scale loops. Consider next that the angular rotation rate at the star’s surface is greater than the Keplerian rate of layers within the inner decretion disk. Magnetic field lines embedded in the disk interact with the stellar field lines, at first gently. They quickly become entangled and stretched because the two fields are anchored to their respective sources. The stretching continues until eventually the lines sever and reconnect. They attempt to come to equilibrium by springing back to a lower magnetic potential and in so doing accelerate particles embedded in them (see Zirker (2012) for a readable discussion of these processes in the solar context). In the  $\gamma$  Cas environment,

they are expected to be accelerated in various directions, including toward the Be star and probably also the disk. Figure 13 depicts this action as a cartoon.

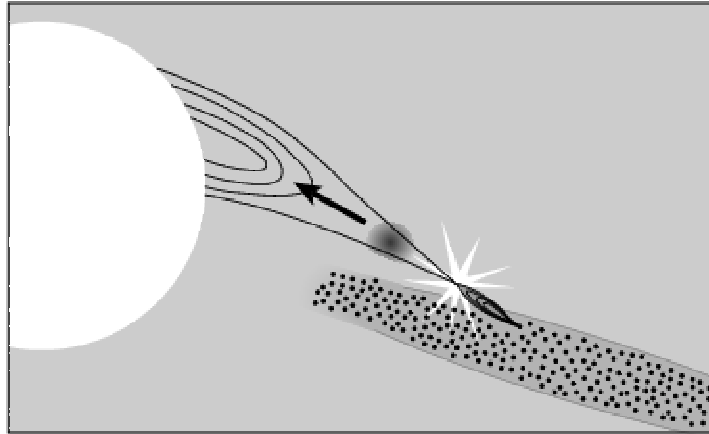


Figure 13: Depiction of the interaction between putative magnetic loop systems from  $\gamma$ Cas and its accretion disk as seen from the equatorial plane. The cartoon shows the acceleration of matter following reconnection of field lines after their initial entanglement and severing. Particle accelerations may be directed toward the star or the disk. After [Robinson & Smith \(2000\)](#).

By hypothesis the field reconnections occur as discrete events, propelling some of the particles toward the star at a few thousand kilometers per second. They impact points on the star, and thermalize there, causing the impacted gas parcels to expand explosively. We interpret these events as X-ray flares. In their analysis of flare dynamics SRC98 showed that the emission measures and durations of the overwhelming fraction of flares expand adiabatically, thereby maintaining their temperature during this expansion phase. Note that SRC98 did not have to specify the source of the high energy.

RS00 took the next step by following the theory of [Wheatland & Melrose \(1995\)](#) and constructing thick target bombardment simulations of electron streams having an energy temperature  $kT$  of 200 keV onto a boundary having parameters of the photosphere of a B star. With these parameters they found a braking depth of the stream that corresponds to a gas density of nearly  $10^{14} \text{ cm}^{-3}$  and a characteristic energy temperature of  $kT \sim 10 \text{ keV}$ . These are precisely the parameters that SRC98 had derived from their observations



of flares for  $\gamma$  Cas. To put some numbers into this concept, consider the case of an exemplar flare with an emission measure of  $10^{55} \text{ cm}^{-3}$ . The flare is formed in an exploding surface parcel with a radius of  $5 \times 10^3 \text{ km}$ . RS00’s high energy (200 keV) electron beam would yield an energy of  $\approx 4 \times 10^{32} \text{ erg s}^{-1}$  across the parcel’s surface. This is sufficient to power the flare for about a second. Note that this is a lower limit because it neglects the high energy tail of the electron distribution that RS00 thought might also be necessary in the real case. It also neglects the virialization of the initial energy of the input beam. Additionally, the value of  $kT_{\text{hot}}$  now generally agreed upon for  $\gamma$  Cas is at least 50% higher than the value of 100 MK (8 keV) RS00 used. Thus, we know the energy numbers of RS00 are low.

This work also demonstrated that an electron beam with a monoenergetic distribution leads to a flare parcel temperature slightly in excess of the temperature of a large magnetically-constrained volume that emits background (basal) flux. If a power law rather than a monoenergetic distribution is assumed for the injected beam, the inequality is reversed:  $T_{\text{flare}} < T_{\text{basal}}$ . Both inequalities have been observed, sometimes within tens of minutes of one another in the X-ray light curves of both  $\gamma$  Cas and HD 110432 (SRC98; SLM12). We remind the reader that the existence of magnetically constrained volumes leading to this basal emission is suggested by the existence of corotating clouds.

If particle streams are directed to the star from instabilities near the inner disk, one can seek to observe them. SR99 reported such evidence in their analysis of spectral time series of 1045 *GHR*S spectra in the March 1996 campaign on  $\gamma$  Cas. These moderate resolution spectra had a very high signal to noise ratio, thereby allowing analyses of variations of even weak spectral lines. The authors constructed a computer program that searched through the time series for similar responses in absorption features separated by wavelength separations corresponding to several pairs of ‘related’ spectral lines. Related line pairs could be members of a multiplet or they might arise from two ions having similar ionization potentials. Cross-correlations were carried out for fluctuations of all spectra in the time series and across a broad velocity domain. The result was a velocity-time map in which ‘excess’ cross-correlations could be identified and compared with correlations for fluctuations at random wavelength spacings, which served as controls. The results showed two interesting patterns. First, the excess cross-correlations occurred, with one exception, only for narrow bands centered at positive velocities. The exception was the strong correlation discovered at a range

of negative velocities for the Si IV resonance line doublet – this is expected for these well-known diagnostics of an outflowing hot-star wind. The second pattern was that the best cross-correlations were found at positive velocities that increased according to the excitation ion state of the lines. For example, for pairs of Fe V and Si IV lines corresponding to a hot gas, excess correlations occurred preferentially for velocities  $\gtrsim +2000 \text{ km s}^{-1}$  while for a pair of low excitation Ni II and S III lines excess correlations occurred for positive velocities of only  $\sim +200 \text{ km s}^{-1}$ . All told, this analysis argued that the excess correlations were real and constitute evidence of high velocity matter expelled toward the Be star. Moreover, velocities of  $>2000 \text{ km s}^{-1}$  are much greater than the escape velocity at the surface of a B0.5 IV star. This fact rules out an interpretation that the features arise as returning matter from an earlier failed ejection. The only reasonable scenario is that the matter had been accelerated toward the star by some intervening structure in our line of sight.

The concept of a disk dynamo was suggested on the basis of the correlation between the optical and X-ray  $\sim 70$  day cycles. To our knowledge this is the first suggestion for a dynamo for any stellar disk. According to this idea, a dynamo is set up in any disk in which the following conditions are met: (1) a seed magnetic field is present within the disk, (2) the angular velocity of the Kepler disk around the star decreases with increasing distance, and (3) no external field intrudes into the disk and disrupts its field. In such disks particle motions will be subject to a magnetorotational instability (MRI), in which a positive feedback loop is set up that increases the disk seed field and gas turbulence. Orbiting gas parcels respond in a dynamo cell by alternately moving inwards and outwards during a cycle (as specific angular momentum does the opposite). During the phase when particles approach their innermost radius, the gas is compressed. This increases the local emission measure, which goes as electron density squared, thereby adding to the luminosity of the star-disk complex. The upshot is that particles and field lines in the inner disk experience cycles, and as they do the instances of entanglement with stellar field lines are modulated as well. This produces cyclic variations in the numbers of accelerated particle streams and generation of flares.

In considering the conditions in which a disk dynamo might operate, a Keplerian rotation law fulfills the orbital velocity-distance requirement. In practice, seed fields can be assumed to exist already (SHV06). The requirement that internal disk fields are not distorted by external ones cannot yet

be evaluated. In evaluating the practicality of this mechanism, the overriding question is not so much whether dynamo actions exist in the disk of  $\gamma$  Cas but rather whether the instabilities of individual cells become organized into a coherent, disk-wide dynamo. Otherwise, local chaotic motions result without a clearly observable global effect. Another issue is that the mechanism is *ad hoc* - it is constructed so far entirely from the phenomenology. However, one clear inference is that energy from magnetic stresses will be periodically exhausted in the inner disk, thereby mediating the production of accelerated particles. In addition, the picture suggests injections of streams distributed at more or less random times such that particles will be accelerated towards all possible longitudes on the Be star surface. Otherwise, quantitative predictions are not yet possible. In particular, the natural period of dynamo cycles is the orbital period of the inner disk, which in this case is no more than a few days, not 70 days. In sum, this hypothesis needs confirmation, including both continued theoretical and laboratory work. It is promising, but it may or may not be the correct instability underlying the observed disk variations. Ultimately, it must be understood why this mechanism would work only for some Be stars.

One can also ask how the magnetic fields on  $\gamma$  Cas might be generated because we know that organized low-order fields do not exist on the star's surface: if they did, their spectral UV resonance lines would show a telltale, regularly changing pattern of emission and absorption features due to clouds frozen into the stellar dipole field. Recent magnetic surveys of Be stars have disclosed that organized, low-order magnetic fields are not detected (Wade et al. 2015). MLS16 have pointed out that of the 18 Be stars for which rotational/disk obliquities are known from Long Baseline Optical Interferometry, the angular rotation rates of  $\gamma$  Cas and HD 110432 are the ones most likely to be close to their critical limits. The effects of destabilizing hydrostatic equilibrium are the greatest in the outer equatorial envelopes of such stars. In the fastest rotating stars the otherwise thin convective envelopes of these stars (which owe their existence to large opacities from Fe peak ions) can increase dramatically (Maeder, Georgy & Meynet, 2008). Therefore, particularly in the case of differential rotation, local dynamos in the stellar envelope could develop that would spawn disorganized, nonpermanent fields – see Cantiello et al. (2009); Cantiello & Braithwaite (2011). Such fields could well elude spectropolarimetric surveys such as Kochukhov & Sudnik (2013), even though their field lines could reach out to the inner regions of the Be disk. While this last argument is speculation, we note from varia-

tions in the waveform of the 1.2-day photometric signature that the surface “patch” corresponding to an embedded structure on the surface of  $\gamma$  Cas has been observed to change on a timescale of two years (HS12). During the same time interval the amplitude of the photometric signature diminished by factor of 3–4. The amplitudes and waveforms were constant to within errors during the few years before and after this interval. However, by the 2013–2014 season the 1.2 day signature was only marginally present in only one of two-filter APT light curves. By the following season it had disappeared altogether (Henry, 2015). These observations are consistent with a constantly-evolving, chaotic, but active field anchored not far under the star’s surface, again following the Cantiello & Braithwaite prescription.

We have no evidence as to how, or indeed whether, the  $\gamma$  Cas stars have been “spun up.” It may be due to a single massive star’s having an especially large angular momentum, or it may be that the spin up occurs from a prior mass transfer thanks to a evolved, now passive degenerate companion. One argument favoring the latter hypothesis is that three of the  $\gamma$  Cas analogs are probably blue stragglers (Table 2). Could most or even all of them be blue stragglers? This is a subject for much more research.

### 6.2.2. *Observational underpinnings of the interaction hypothesis.*

We recapitulate this section by listing the observational underpinnings of the magnetic star-disk interaction picture. Most of these have been introduced already. We summarize them in rough order of their chronology of the discovery that the star is a hard X-ray source.

1. X-ray correlations/anticorrelations are evident in the intermediate-timescale variations of UV diagnostics. The key point is that in the Be/disk/binary complex only the Be star emits enough UV continuum and line fluxes for variations to be easily observed. The time coverage of the simultaneous 1996 *RXTE/HST* observations was too long (Figs. 5–7), and both the number of up/down flux excursions and the pattern too self-consistent, to have occurred by chance. One concludes that the X-rays are created close to the Be star.
2. X-ray flares of  $\gamma$  Cas and HD 110432 must be emitted in a high density ( $\gtrsim 10^{14}$  cm $^{-3}$ ) environment. This limit is set by their short lifetimes (§3.1.4) and the ratios of spectral emission lines arising from Fe L-shell ions (§2.3). Only the photospheres of the two binary components could be the site of these flares. From the consideration of Bullet 1 one is left with the Be photosphere as the site of flare production.

3. An attenuation of soft X-rays was observed that coincided precisely with the optical Be outburst of  $\gamma$  Cas in 2010 (§3.8 and Figure 3). As this outburst proceeded over the 40 days of the *XMM* observations, the spectra showed progressive attenuations of the soft X-ray flux, thereby requiring an increased local absorption column  $N_{\text{H}_b}$  to fit the spectrum. At visible wavelengths, an optical outburst generally unfolds as a brightening and reddening of the flux from the star-disk complex. Again, Figure 12 showed the relation between  $(B - V)$  color and the determined  $N_{\text{H}_b}$  column. The figure overplots the same parameters during the 2001 and 2004 X-ray observations, so we can see a common relation between these variables during different these times. Because the emission of the hot primary plasma dominates at both short and long X-ray wavelengths, the column obscuring the soft X-rays also obscures hot X-ray emitting sites in the background. Since the column represents an injection of matter from the Be star to its circumstellar environment, this pattern indicates that the hot plasma sources are situated at the foot of the column, i.e., just above or even at the surface of the Be star.
4. No delays are observed in integrated X-ray variability relative to optical variations of  $\gamma$  Cas. The MLS15 extension of the RSH02 and SHV06 work that the scalings of correlated X-ray and optical variations over a timescale from tens of days to a year or so is important because it demonstrates that only a small (dense inner) region of the  $V$ -emitting decretion disk is involved in the optical/X-ray correlations. MLS15 also investigated the possibility that discrete Be ejections could transit across the binary system and accrete onto a degenerate companion such as a WD. However, they recognized that such ejecta would take a finite time to travel past the outer truncation and Roche lobe radii before falling onto the putative WD. These authors found no delay in the X-ray variations behind the optical ones. Using Monte Carlo techniques to noise to their *APT* and *ASM* data, the authors estimated errors on this null result of one month. In contrast, they pointed out that two well known X-ray Be binary systems with comparable orbital separations are *observed* to show a delay of a few years of X-ray responses following optical outbursts of the Be primaries. On this basis, the authors argued that any X-ray generation mechanism requiring accretion onto a degenerate secondary in the orbit known for the  $\gamma$  Cas companion is inadmissible.

5. Long-cycle variations are mediated by conditions in the inner part of the Be disk. The good correlation of X-ray and optical long cycles noted by SHV06 and MLS15 demonstrates that the circumstellar Be disk is somehow *associated* with X-ray generation. According to the star-disk interaction scenario, the disk provides a storage medium for pent up magnetic energy that is released at semi-periodic intervals. In this sense it represents an intermediate link in a chain of processes leading to particle acceleration and ultimately X-rays.

## 7. Summary & Conclusions.

### 7.1. Summary.

In this paper we have reviewed the study of X-ray properties of  $\gamma$  Cas to date. Work over the last several years has clarified that this star is actually the prototype of a class of peculiar X-ray emitters among those associated with massive hot stars. To the extent that observations of fainter stars can unveil them, these studies reveal remarkably similar properties in the X-ray, UV, and optical domain. Part of this review has been an evaluation of candidate mechanisms for the emission of the hard X-rays, including one in which accretion onto a degenerate companion, with its deep gravitational well, could release X-rays.

The Be-NS scenario, favored for a decade or more after [White et al. \(1982\)](#), became disfavored following a consensus that the X-ray spectrum can be fit not by a sum of black body spectrum with an additional nonthermal (Compton) tail but rather by the combined emission of multi-component, optically thin thermal plasmas. In particular, emission lines from the FeK complex at  $\lesssim 2 \text{ \AA}$  and others arising from light-element ions in the soft X-ray regime are present in the spectra of  $\gamma$  Cas stars. In addition, the X-ray light curves of Be-NS systems are dominated either by strictly periodic pulses, as in highly magnetized Be X-ray pulsar systems, or semi-regular outbursts tied either to the orbital period or unpredictable optical Be star events.

It took some additional time for a consensus (albeit perhaps still not unanimous) to arise that the Be-WD systems cannot fit the observed multi-band phenomenology. It is still the case that the efficiencies of mass transfer and thermalization must be exquisitely fine-tuned to match the X-ray luminosities of these systems, particularly with what we now understand the mass loss rates of  $\gamma$  Cas and other classical Be stars to be. Furthermore, searches for Be-WD systems have consistently come up either as altogether negative

(Güdel & Nazé, 2009) or as hypothetical suggestions of special cases, such as super-soft X-ray systems, that do not mimic the X-ray characteristics of  $\gamma$  Cas stars. In addition, the simultaneous array of multi-component thermal plasmas with ubiquitous, “gray” flaring are attributes that are rare in active WD systems, if present at all.

The strongest arguments for the magnetic star-disk interaction picture - which is undoubtedly incomplete at some level - are corroborative, rather than exclusionary. As detailed in §6.2.2 these arguments pertain to X-ray variations and their correlations on a wide variety of timescales with UV or optical diagnostics. Here it should be understood that these diagnostics are to be expected to be formed over the surface of a  $\sim$ B0.5 star.

In the following we will pose the most relevant questions that can at last be asked about this class of stars. We follow with a few desiderata on what needs yet to be done. We do this with trepidation because the history of this subject has been that progress has often come from very unexpected sources.

### *7.2. Questions, resolved or nearly so.*

#### *Can we easily recognize a $\gamma$ Cas star?*

In principle, yes. Given that optical spectra show that an early B star is a Be star neither embedded in a star-forming region or a component of an interacting binary, the work of L07a and G15 have strongly suggested that if its X-ray spectrum exhibits the full FeK line complex and a nearby continuum slope that supports the energy temperatures (i.e.,  $\gtrsim 7$  keV) needed to maintain the strength of these lines as well as an  $L_X$  of  $10^{32}$ - $10^{33}$  ergs  $s^{-1}$ , the star may be reasonably advanced as a  $\gamma$  Cas analog. These circumstances favor a wholesale discovery that has been so successful in the last few years in expanding the class, particularly thanks to cross-correlations of *XMM/EPIC* surveys with optical or even infrared catalogs. The sample as now recognized is probably complete out to a distance of  $\sim 2$  kpc, at least for the area covered by the *XMM* surveys. The coverage can be furthered by continued cross-correlation of hard X-ray and infrared catalogs in the Galactic plane.

#### *Do we have a large enough sample of $\gamma$ Cas stars yet to constrain the range of their X-ray characteristics?*

From the sample of stars in Table 2 we now have a well defined parameter space which helps to constrain the X-ray generation mechanism resides. Some areas where improvement could be required are covered by the following questions: can a late-type Oe star assume the X-ray properties of  $\gamma$  Cas stars

during the much briefer times their decretion disks are maintained? Is there truly no overlap at B2 with the Bp stars, where both ordered and disordered fields could exist simultaneously on a star’s surface? Also, what is the lowest energy temperature an X-ray plasma hosted by in a  $\gamma$  Cas star may have? At the moment it appears to be about 6–7 keV. The physical conditions setting this limit will be relevant to understanding the geometry and magnetic topology of the X-ray producing environment, possibly including the status of the Be inner disk.

### *7.3. Desiderata.*

A primary issue to resolve is the role of binarity in the setting up of the X-ray generation mechanism in  $\gamma$  Cas stars. This question comes up first because of the known binarity of  $\gamma$  Cas itself and second because of the likelihood that at least three analogs are old blue stragglers in Galactic clusters. An answer to this question will disclose critical details about their past evolution, their current intrabinary interactions and, most especially, whether binarity is an essential element that causes the Be star to spin up to criticality. Thus, we recommend radial velocity monitoring in order to define the binary status of  $\gamma$  Cas stars – the only known  $\gamma$  Cas binary so far being  $\gamma$  Cas itself. The questions to be asked are: what are the ranges in semimajor axes and orbital eccentricities?

We have speculated that an early Be star’s rotating at near the critical velocity is important in setting up local envelope dynamos that create unstable local magnetic fields. There are three approaches to test this idea. The first is to explore the efficacy of diffusing excess angular momentum deposited on the star’s surface by transfers of matter from a putative companion. This question can be addressed theoretically or by an empirical study of angular rates inside a B star determined from rotational splitting of nonradial pulsation modes. The second approach is to address the critical rotation question observationally by confirming that a near-critical rotation rate is important to the creation of the needed surface conditions for the mechanism to develop, as suggested by MLS15. Improvements in LBOI instrumentation (or increases in the total integration time) would help refine estimates in the obliquity angles of the rotation planes of some of the brighter analogs.

The third approach is to survey binarity of a bright subsample of  $\gamma$  Cas analog stars from long-term studies of their radial velocity curves. For example, a single, compelling nondetection of a nonvariable RV curve of an  $\gamma$  Cas suspected to viewed edge-on (from the presence of double-peaked emission



profile as well as absorption “shell” lines) would go a long way to refuting the question of binarity.

The report by [Henry \(2015\)](#) that the rotational signature in the light curve of  $\gamma$  Cas has disappeared now invites the expectation that it will return. Further APT observations will tell us how long it takes to reappear, grow to full strength and indeed whether the patch responsible for it will reemerge on the surface at the same place (longitude).

A remaining important question is whether the presence of a stable Be decretion disk, as measured by some minimum EW of H $\alpha$  emission, is indeed necessary for the production of hard X-rays. Over the coming period, whether it be measured in years or a few decades, astronomers should be able to monitor the H $\alpha$  variability enough to catch the transition of one of the  $\gamma$  Cas stars in Table 2 as it slips into a non-Be phase. When this happens it will be of great interest to verify whether the X-ray emission quickly subsides and, assuming this to be so, to examine how the specific spectroscopic X-ray diagnostics change during the transition to the quiet phase.

Our final rhetorical question is whether a search for faint reflection and emission nebulae similar to IC 59 and IC 63, which are spatially correlated with  $\gamma$  Cas ([Poeckert & van den Bergh, 1981](#)), might reveal nebulosities in the disk planes of other  $\gamma$  Cas stars. One wonders: are such nebulosities common around  $\gamma$  Cas stars but absent from other active Be stars? In addition, these authors suggested that a light echo could be observed in such nebulae some years after a large optical outburst of the Be star (as would be expected now after three years in the case of  $\gamma$  Cas).

All these investigations are aimed at answering the key question: how does the hard X-ray emission from  $\gamma$  Cas star form? Clearly the development of the “ $\gamma$  Cas phenomenon” requires the emergence of a complicated chain of processes. We have identified a number of observational disciplines and studies that are necessary for this development. They include X-ray and optical spectroscopy and photometry, Long Baseline Optical Interferometry, as well as a comparison of characteristics of  $\gamma$  Cas analogs to accretion-related phenomena known to occur on other evolved binary systems. However, these disciplines alone are unlikely to reveal the *linkages* in the chain of processes that produce hard X-rays, and so new ones will be needed. Foremost among them will be theoretical investigations, especially of magnetic dynamos in the envelopes and disks of Be stars. These can lead to requirements for their maintenance and predictions of their durability.

We wish to thank Dr. Gerrie Peters and Chris Shrader for helpful conversations and for Chris's permission to use a modified figure in this paper. We express our great appreciation to two conscientious referees, as well as to our editor, Dr. Lida Oskinova, for a careful reading. Each of these professionala have provided comments that have led to improvements of this review. R.L.O. was supported by the Brazilian agencies CNPq (Universal Grants 459553/2014-3) and INCTA (CNPq/FAPESP)

## 8. Citations

### References

- Apparao, K. M., The spin period and orbital relation for Be star/white dwarf binary systems, *A&A*, 291, 775-776A, 1994.
- Apparao, K. M., Support for a white dwarf in the Be star  $\gamma$  Cassiopeiae, *A&A*, 382, 554-555A, 2002.
- Aschwanden, M. J., *Self Organized Criticality* (Berlin: Springer), ISBN-978-3-642-15000-5, Ch. 13.2.5–13.2.6, 2011.
- Beardmore, A. P., & Osborne, J. P., Simultaneous rapid hard X-ray and optical variability in AM Herculis, *MNRAS*, 290, 145-159B, 1997.
- Berio, P., Stee, Ph., Vakili, F., et al., Interferometric insight into gamma Cassiopaeiae long-term variability, *A&A*, 345, 203-210S, 1999.
- Cameron-Collier, A., & Robinson, R. D., Fast H-alpha variations on a rapidly rotating cool main sequence star, *MNRAS*, 236, 57-87C, 1989.
- Cantiello, M., & Braithwaite, J., Magnetic spots on hot massive stars, *A&A*, 540A, 140-147C, 2011.
- Cantiello, M., Langer, N., Brott, I., et al., Sub-surface convection zones in hot massive stars and their observable consequences, *A&A*, 499 279C, 2009.
- Codina, S. J., de Freitas Pachero, J. A., Lopes, D. F., et al., The spectrum of the Be star HD 110432, *A&AS*, 57, 239-247C, 1984.
- Cohen, D. H., X-ray emission from isolated Be stars, in *The Be Phenomenon in Early-Type Stars*, ed. M. Smith, H. Henrichs, & J. Fabregat, ASP Conf. Ser., 175, 156-169C, 2000.

- Corbet, R. H. D., & Mason, K. O., The optical counterpart of 3A0726-260 (4U0728-25), *A&A*, 131, 385-389C, 1984.
- Corral, A., Georgantopoulos, I. & Watson, M., The XMM-Newton Spectral Fit Database, in *The X-ray Universe 2014*, ed. J.-U. Ness, in press; online at [http://xmm.esac.esa.int/external/xmm\\_science/workshops/2014symposium/](http://xmm.esac.esa.int/external/xmm_science/workshops/2014symposium/), 2014.
- Cranmer, S. R., Smith, M. A., & Robinson, R. D., The Case for Illuminated disk-enhanced wind streams in  $\gamma$  Cassiopeiae, *ApJ*, 537, 433-447C, 2000.
- Doazan, V., Franco, M., Sedmak, G., et al., The log-term variations of gamma Cas in the visual, *A & A*, 128, 171-180D, 1983.
- Frontera, F., Dal Fiumi, D., Robba, N. R., et al., The variability of gamma Cassiopeiae in X-rays, *ApJ*, 320L, 127-131F, 1987.
- Gies, D. R., Bagnuolo, W. G., Baines, E. K., et al., CHARA array K'-band measurements of the angular dimensions of Be star disks, *ApJ*, 654, 527-543G, 2007.
- Giménez-García, A., Torrejón, J. M., Eikmann, W., et al., An XMM-Newton view of Fe K $\alpha$  in HMXBs, *A&A*, 576A, 108-138G 2015, (G15).
- Güdel, M. & Nazé, Y., X-ray spectroscopy of stars, *A&A Rev*, 17, 309-406G, 2009.
- Haberl, F., *A&A*,  $\gamma$  Cassiopeiae: evidence for a Be star/white dwarf X-ray binary?, 296, 685-690H, 1995.
- Hanuschik, R. W. & Vrancken, M., Shell lines in 48 Lib, *AA*, 312, L17-20H, 1996.
- Harmanec, P., Habuda, P., Štefl, S., et al., Binary nature and orbital elements of gamma Cas, *A&A*, 364, L85H, 2000.
- Harmanec, P., Strange among the strange: the B-emission star  $\gamma$  Cassiopeiae, in *Exotic Stars as Challenges to Evolution*, ed. C. A. Tout & W. Van Hamme, *ASP Conf. Ser.*, 279, 221-237H, 2000.
- Henry, G. W. 2015, priv. commun.

- Henry, G. W., & Smith, M. A., Rotational and cyclical variability in  $\gamma$  Cassiopeiae, *ApJ*, 760, 10-21H, 2012.
- Horaguchi, T., Kogure, T., Hirata, R., et al., The Be star  $\gamma$  Cassiopeiae: observations in 1989, *PASJ*, 46, 9-26H, 1994. *MNRAS*, 296, 949-960H, 1998.
- Hummel, W., On the spectacular variations of Be stars. Evidence for a temporarily tilted circumstellar disk, *A&A*, 330, 243-252H, 1998.
- Jernigan, G., MX1803-24, IAUC No. 2900, 1976.
- Jones, C., E., Wiegert, P. A., Tycner, C. et al., Using photometry to probe the circumstellar environment of  $\delta$  Scorpii, *ApJ*, 145, 142-148J, 2013.
- Kahabka, P., Haberl, F., Payne, J. L., et al., Supersoft sources in XMM-Newton Small Magellanic Cloud fields, *A&A*, 458, 285-292K, 2006.
- Kahabka, P., van den Heuvel, E. P., Luminous supersoft X-ray sources, *ARA&A*, 35, 69-100, 1997.
- Knigge, C., Coe, M. J., & Podsiadlowski, P., Two populations of X-ray pulsars produced by two types of supernova, *Nature*, 479, 372K, 2011.
- Kubo, S., Murakami, T., Ishida, M., et al., ASCA X-ray observations of gamma Cassiopeiae, *PASJ*, 50, 417-426K, 1998 (K98).
- Kochukhov, O., & Sudnik, N., Detectability of small-scale magnetic fields on early-type stars, *A&A*, 554, A93-102K, 2013.
- Laming, J. M., A unified picture of the First Ionization Potential and Inverse First Ionization Potential effects, *ApJ*, 614, 1063-1072L, 2004.
- Laming, J. M., Non-Wkb models of the First Ionization Potential effects, *ApJ*, 695, 954-969L, 2009.
- Lopes de Oliveira, R., A new class of X-ray emitters: the  $\gamma$  Cassiopeiae-like sources, Univ. de São Paulo, Brazil, 2007 (L07a).
- Lopes de Oliveira, R. & Motch, C., Hard X-ray emission from the massive emission-line star, HD 157832, *ApJ*, 731L, 6-9L, 2011.

- Lopes de Oliveira, Motch, C., Haberl, F., et al., New  $\gamma$  Cassiopeiae-like objects: X-ray and optical observations of SAO 49725 and HD 161103 A&A, 454, 265-276L, 2006 (L06).
- Lopes de Oliveira, R., Motch, C., Smith, M. A. et al., On the X-ray and optical properties of the Be star HD 110432, A&A, 474, 983-996L, 2007 (L07b).
- Lopes de Oliveira, R., Smith, M. A., & Motch, C. ,  $\gamma$  Cassiopeiae: an X-ray Be star with personality, A&A, 512, A22-33L, 2010 (L10).
- Maeder, A., Georgy, C., & Meynet, G., Convective envelopes in rotating OB stars, A&A, 479, L37-40M, 2008.
- Marco, A., Negueruela, I., & Motch, C., Blue stragglers in young open clusters, in Massive Stars in Interacting Binaries, eds. N. St.-Louis & A. Moffat, ASP Conf. Ser., 367, 645-651M, 2007.
- Marco, A., Negueruela, I., Ribó, M., et al., Blue stragglers, Be stars, and X-ray binaries in open clusters, Adv. Sp. Res., 44, 348-354M, 2009.
- Marlborough, J. M., Gamma Cassiopeiae and the transient X-ray source MX0053+60, PASP, 89, 122-126M, 1977.
- Martins, F., Schaerer, D., & Hillier, D. J., On the effective temperature scale of O stars, A&A, 382, 999-1004M, 2002.
- Martinez Riberio, E., Lopes de Oliveira, R., Motch, C., et al., An optical spectroscopic campaign of southern  $\gamma$  Cas analogs, in The X-ray Universe 2014, ed. J-W Ness, 283M; abstract at <http://adsabs.harvard.edu/abs/2014xru..confE.283M>, 2014.
- Mauche, C. W. & Liedahl, D. A., & Fournier, K. B., Application of the FeXVII I(17.10Å)/I(17.05)Å ratio to constrain the plasma density of an X-ray source, ApJ, 560, 992-996M, 2001.
- McSwain, J., & Gies, D. R., The evolutionary status of Be stars: southern open clusters, ApJS, 161, 118-146M, 2005.
- Meilland, A., Delaa, O., Stee, Ph., et al., The Be star binary  $\delta$  Scorpii at high spectral and spatial resolution, A&A, 532, A80-89M, 2011.

- Miroshnichenko, A. S., Bjorkman, K., & Krugov, V. D., Binary and long-term variations of  $\gamma$  Cassiopeiae, *PASP*, 114, 1226-1233M, 2002.
- Millar, C. E., Sigut, A. A., & Marlborough, J. M., New insights on Be shell stars from modeling their  $H\alpha$  emission profiles, *MNRAS*, 312, 465-469A, 2000.
- Motch, C. 2015, priv. commun.
- Motch, C, Haberl, F., Dennerl, K., et al., New massive X-ray binary candidates from the ROSAT Galactic Plane Survey, *A&A*, 323, 853-875M, 1997.
- Motch, C., Herent, O., & Guillout, P., The source content of low galactic XMM-Newton surveys, *Astr. Nachr.*, 324, 61-64M, 2003.
- Motch, C., Lopes de Oliveira, R., Negueruela, I., et al., X-ray and optical properties of new gcas-like objects discovered in X-ray surveys, in *Active OB Stars*, ed. S. Štefl, S. Owocki, & A. Okazaki, *ASP Conf. Ser.* 361, 117-123M, 2007 (M07).
- Motch, C., Lopes de Oliveira, R., & Smith, M. A., The origin of the puzzling X-ray emission of  $\gamma$  Cassiopeiae, *ApJ*, 806, 177-186M, 2015 (MLS15).
- Motch, C., Warwick, R., Cropper, M. S., et al., The X-ray source content of the XMM-Newton Galactic plane survey, *A&A*, 523, A92-131M, 2010.
- Motch, C., Herent, O, & Guillout, P., The source content of the low galactic latitude XMM-Newton surveys *AN*, 324, 61-64M, 2003.
- Mouchet, M., Bonner-Didaud, J., & de Martino, D., The X-ray emission of magnetic cataclysmic variables in the XMM-Newton era, *Mem. Soc. Astron. Ital.*, 83, 578-584M, 2012.
- Murakami, T., Koyama, K., Inoue, H., et al., X-ray spectrum from gamma Cassiopeiae, *ApJ*, 310, L31-34M, 1986.
- Nebot Gómez-Morán, A., Motch, C., Barcons, X., et al., The XMM-Newton SSC survey in the Galactic plane, *A&A*, 553, A12-32N, 2013 (N13).

- Nebot Gómez-Morán, A., Motch, C., Barcons, X., et al., Infrared identification of hard X-ray sources in the Galaxy, MNRAS, 452, 884N, 2015 (N15).
- Nemravová, J., Harmanec, P., Koubska, P., et al., Orbital and long-term spectral variations of  $\gamma$  Cassiopeiae, A&A, 537, 59-69N, 2012.
- Okazaki, A., Bate, M. R., Ogilvie, G. I., et al., Viscuous effects on the interaction between the coplanar decretion disc and the neutron star in Be/X-ray binaries, MNRAS, 337, 967-980O, 2002.
- Okazaki, A., & Negueruela, I., A natural explanation for the periodic X-ray outbursts in Be/X-ray binaries, A&A, 377, 161-174O, 2001.
- Owens, A., Osterroek, T., Parmar, A. N., et al., BeppoSAX broad-band observations of gamma Cassiopeiae, A&A, 348, 170-174O, 1999.
- Parmar, A. N., Israel, G. I., Stella, L., et al., The X-ray time variability and spectrum of  $\gamma$  Cassiopeiae, A&A, 275, 227-235P, 1993.
- Peters, G. J., The hard X-ray flux from gamma Cassiopeiae during 1970-73, PASP, 94, 157-161P, 1982.
- Poekert, R., & van den Bergh, S., The gamma Cassiopeiae nebulae, PASP, 93, 703-706P, 1981.
- Pollmann, E., Vollmann, W., & Henry, G. W., Long-term monitoring of H $\alpha$  emission strength and photometric V magnitude of gamma Cas, in Info. Bull. on Var. Stars, 6019, 1-1, 2014.
- Quirrenbach, A., Bjorkman, K. S., Bjorkman, J. E., et al., Optical interferometric and spectropolarimetric observations of seven Be stars, ApJ, 479, 477Q, 1997.
- Raguzova, N. V., Population synthesis of Be/white dwarf binaries in the Galaxy, A&A, 367, 848-858R, 2001.
- Rakowski, C. E., Schulz, N. S., Wolk, S. J., et al., Extraordinarily hot X-ray emission from the O9 emission-line star HD 119682, ApJ, 649, L111-114R, 2006 (R06).

- Rauw, G., Naze, Y., Spano, M., et al., HD 45314: a new  $\gamma$  Cassiopeiae analog among Oe stars, *A&A*, 555, L9-12R, 2013.
- Robinson, R. D., & Smith, M. A., A search for rotational modulation of X-ray centers on the classical Be star  $\gamma$  Cassiopeiae, *ApJ*, 540, 474-488R, 2000 (RS00).
- Robinson, R. D., Smith, M. A., & Henry, G. W., X-ray and optical variations in the classical Be star  $\gamma$  Cassiopeiae, *ApJ*, 575, 435-448R, 2002, (RSH02).
- Safi-Harb, S., Ribó, M., Butt, Y., et al., A multiwavelength study of 1WGA J1346.5-6255, *ApJ*, 659, 407-418S, 2007 (SH07).
- Samus, N. N., Durlevich, O. V., et al., General catalog of variable stars (Samus+2007-2013), *VizieR yCat....102025S*, 2009.
- Schwarz, R., Reinsch, K., Beuermann, K., et al., XMM-Newton observation of the long-period polar V1309 Orionis, *A&A*, 442, 271-279S, 2005.
- Secchi, A., Schreiben des Herrn Prof. Secchi an den Herausgeber, *Astron. Nachr.* 68, 63-64, 1866.
- Shrader, C. R., Hamaguchi, K., Sturmer, S. J., et al., High-energy properties of the enigmatic Be star  $\gamma$  Cassiopeiae, *ApJ*, 799, 84-91S, 2015.
- Sigut, T. A., & Jones, C. E., The thermal structure of the circumstellar disk surrounding the classical Be star  $\gamma$  Cassiopeiae, *ApJ*, 668, 481-491S, 2007.
- Slettebak, A., & Snow, T. P., J., Simultaneous ultraviolet and H-alpha observations in the Be star gamma Cassiopeiae, *ApJ*, 224, L127-131S, 1978.
- Smith, M. A., Rapid multiwavelength variability in gamma Cassiopeiae, *ApJ*, 442, 812-821S, 1995.
- Smith, M. A., and Balona, L. A., The remarkable Be star HD 110432, *ApJ*, 640, 491-504L, 2006.
- Smith, M. A., Cohen, D. H., Gu, M., et al., High-resolution Chandra Spectroscopy of  $\gamma$  Cas, *ApJ*, 600, 972-985S, 2004 (S04).
- Smith, M. A., Henry, G. W., & Vishniac, E., Rotational and cyclical variability in  $\gamma$  Cassiopeiae, *ApJ*, 647, 1375-1386S, 2006 (SHV06).



- Smith, M. A., & Robinson, R. D., The case for magnetically controlled circumstellar kinematics in  $\gamma$  Cassiopeiae, *ApJ*, 517, 866-882S, 1999 (SR99).
- Smith, M. A., & Robinson, R. D., Periods, cycles, and chaos in the high-energy emissions of gamma Cas, in *Interplay of Periodic, Cyclic & Stochastic Variability*, ed. C. Sterken, ASP Conf. Ser., 292, 263-273, 2003 (SR03).
- Smith, M. A., Robinson, R. D., & Corbet, R. H. D., The case for surface X-ray flaring on  $\gamma$  Cassiopeiae, *ApJ*, 503, 877-893S, 1998a, (SRC98).
- Smith, M. A., Robinson, R. D., & Hatzes, A. P., The case for corotating circumstellar clouds on  $\gamma$  Cassiopeiae, *ApJ*, 507, 945-945S, 1998 (SRH98).
- Smith, M. A., Lopes de Oliveira, R., & Motch, C., Characterization of the X-ray light curve of the  $\gamma$  Cas-like B1e star HD 110432, *ApJ*, 755, 64-74S, 2012 (SLM12).
- Smith, M. A., Lopes de Oliveira, R., Motch, C. et al., The relationship between  $\gamma$  Cassiopeiae's X-ray emission and its circumstellar environment, *A&A*, 540, A53-68S, 2012 (S12).
- Smith, M. A., Lopes de Oliveira, R., & Motch, C., Turning the tide: the origin of hard X-rays from  $\gamma$  Cas, in *ASPC Ser.*, ed. A. Sigut & C. Jones, in press, 2015 (SLM15).
- Sota, A. Maíz Apellániz, J, Walborn, N. R. et al., The Galactic O-Star Survey. I. Classification System, *ApJS*, 193, 24-73S, 2011.
- Stee, Ph., On the kinematics of the envelope of  $\gamma$  Cassiopeiae, *A&A*, 311, 945-950S, 1996.
- Stee, Ph., Delaa, O., Monnier, R. D., et al., Geometry and kinematics of the disk of  $\gamma$  Cas from MIRC and VEGA instruments on the CHARA array, *A&A*, 545, 59-73A, 2012.
- Steele, I. A., & Clark, J. S., A representative sample of Be stars III: H-band spectroscopy, *A&A*, 371, 643-651S, 2001.
- Sturm, R., Haberl, F., Pietch, W., et al. A new super-soft X-ray source in the Small Magellanic Cloud: Discovery of the first Be/white dwarf system in the SMC?, *A&A*, 537, A76-81S, 2012.

- Telting, J. H. & Kaper, L. , Long-term variability in UV absorption lines of the Be star gamma Cassiopeiae, *A&A*, 284, 515-529T, 1994.
- Thom, C., Granès, P. & Vakili, F. Optical interferometric measurements of gamma Cassiopeiae's envelope in the H-alpha line, *A&A*, 165, L13-15T, 1986.
- Torrejón, J. M. & Orr, A., BeppoSAX survey of Be/X-ray binary candidates, *A&A*, 377, 148-155T, 2001.
- Torrejón, J. M., Schulz, N. S., & Nowak, M. A., Chandra and Suzaku Observations of the Be/X-ray star HD 110432, *ApJ*, 750, 75-81T, 2012 (TSN12).
- Torrejón, J. M., Schulz, N. S., & Nowak, M. A., et al., Hot Thermal X-ray emission from the Be Star HD 119682, *ApJ*, 765, 13-17T, 2013 (T13).
- Tycner, C., Gilbreath, G. C., Zavala, R. T., et al., Constraining disk parameters of Be stars using narrowband H $\alpha$  interferometry with the Navy Prototype Optical Interferometry, *AJ*, 131, 2710-2721T, 2006.
- van Leeuwen, F., Hipparcos: the new reduction of the raw data, *Astrophys. Space Sci. Lib. (Springer)*, 350, 3-37, 2007.
- Wade, G., Petit, V., Grunhut, J., et al., The MiMes survey of magnetism in massive stars, introduction and overview, arXiv:1411.6165, 2016. C. Jones, Bright Emissaries Conference, ASP Conf. Ser. ed. A. Sigut & C. Jones, in press, 2015.
- Wheatland, M. S., & Melrose, D. B., Interpreting YOHKOH hard and soft X-ray flare observations, *Sol. Phys.*, 158, 283-299W, 1995.
- White, N. E., Swank, J. H., Holt, S. S., et al., A comparison of the X-ray properties of X Persei and gamma Cassiopeiae, *ApJ*, 263, 277-288W, 1982.
- Yang, S., Ninkov, Z., Walker, G. A., Nonradial oscillations in the Be star gamma Cassiopeiae, *PASP*, 100, 233-242Y, 1988.
- Zirker, J. B., The Violent Sun (Chapter 4), in *The Magnetic Universe*, Johns Hopkins Univ. Press, 2012.